The anterior Hox gene *ceh-13* and *elt-1/GATA* activate the posterior Hox genes *nob-1* and *php-3* to specify posterior lineages in the *C. elegans* embryo

John Isaac Murray[2], Elicia Preston[2], Jeremy P. Crawford[1], Jonathan D. Rumley[2], Prativa Amom[1], Breana D. Anderson[1], Priya Sivaramakrishnan[2], Shaili D. Patel[2], Barrington Alexander Bennett[2], Teddy D. Lavon[2], Felicia Peng[2], Amanda L. Zacharias[1,3,4]

1. **Division of Developmental Biology, Cincinnati Children's Hospital Medical Center, Cincinnati, OH 45229**
2. **Department of Genetics, Perelman School of Medicine, University of Pennsylvania, Philadelphia, PA 19104**
3. **Department of Pediatrics, University of Cincinnati College of Medicine, Cincinnati, OH 45267**
4. **Corresponding author - *Amanda.Zacharias@cchmc.org***

Abstract

Hox transcription factors play a conserved role in specifying positional identity during animal development, with posterior Hox genes typically repressing the expression of more anterior Hox genes. Here, we dissect the regulation of the posterior Hox genes *nob-1* and *php-3* in the nematode *C. elegans*. We show that *nob-1* and *php-3* are co-expressed in gastrulation-stage

embryos in cells that previously expressed the anterior Hox gene *ceh-13*. This expression is controlled by several partially redundant transcriptional enhancers. These enhancers require *ceh-13* for expression, providing a striking example of an anterior Hox gene positively regulating a posterior Hox gene. Several other regulators also act positively through *nob-1/php-3* enhancers, including *elt-1/GATA*, *ceh-20/ceh-40/Pbx*, *unc-62/Meis*, *pop-1/TCF*, *ceh-36/Otx* and *unc-30/Pitx*. We identified defects in both cell position and cell division patterns in *ceh-13* and *nob-1;php-3* mutants, suggesting that these factors regulate lineage identity in addition to positional identity. Together, our results highlight the complexity and flexibility of Hox gene regulation and function and the ability of developmental transcription factors to regulate different targets in different stages of development.

Author Summary

Hox genes are critical for head-to-tail patterning during embryonic development in all animals. Here we examine the factors that are necessary to turn on two posterior Hox genes, *nob-1* and *php-3*, in the nematode worm, *C. elegans*. We identified six new transcription factors and three enhancer regions of DNA that can activate expression of *nob-1/php-3*. Unexpectedly, these activating transcription factors included *ceh-13*, an anterior Hox gene, and *elt-1*, a regulator of skin development that is briefly expressed in many cells that do not adopt skin fates, including the cells that express *nob-1*. Furthermore, the cellular defects we observed in *ceh-13* and *nob-1;php-3* mutant embryos indicate that the early embryonic functions of these Hox genes help determine the identity of cells as well as their position within the embryo. Our findings identify new roles for Hox genes in *C. elegans* and emphasize the ability of transcription factors to contribute to the diversification of cell types and the adoption of specific cell types at different phases of embryonic development.

Introduction

Hox genes are conserved transcription factors famously expressed in specific positions along the anterior-posterior axis during animal development that specify axial position. Mutations in Hox genes cause a wide variety of developmental defects in both model organisms and humans. Hox gene regulation is complex and includes both transcriptional and post-transcriptional control. In most animals, Hox genes are found in genomic clusters, and their expression along the A-P axis is collinear with their genomic position, and often show "posterior dominance," where posterior Hox genes repress the expression of more anterior Hox genes (Reviewed in (1–3)).

The genome of the nematode *Caenorhabditis elegans* encodes a single set of six Hox genes on Chromosome III, loosely organized into three degenerate "clusters" that each contain two adjacent genes (4–6,3). The cluster containing *lin-39* and *ceh-13* is inverted relative to Hox clusters in other organisms as *ceh-13*, a homolog of *HoxA1/labial,* is downstream of *lin-39,* a homolog of *HoxA4/Deformed*(7–9). In larval stages, these genes are expressed in specific positions along the A-P axis and regulate both positional differences in cell fate and function, similar to their homologs in other animals (10–18), and directly regulate terminal fates (19).

Three of these, the anterior Hox gene homolog *ceh-13/HOX1* and the posterior Hox gene homologs *nob-1/HOX9-13* and *php-3/HOX9-13,* are also expressed in early embryogenesis, during gastrulation (5,20–22). *ceh-13* mutants have severe defects in anterior (head) morphology(21), while mutants lacking both *nob-1* and *php-3* have severe posterior (tail) defects(5). Partial cell lineage tracing of *ceh-13* and *nob-1*;*php-3* mutants identified defects in cell position but not in division patterns, leading to the hypothesis that these genes regulate positional identity, rather than lineage identity(5,6,21).

Intriguingly, despite their apparently opposite roles in anterior vs posterior morphogenesis, both *ceh-13* and *nob-1* are expressed in overlapping posterior lineages during gastrulation and both require the Wnt pathway for this expression(23,24). *ceh-13* is transiently expressed in the progeny of 7 of the 8 posterior sister cells derived from the (largely ectoderm-producing) AB blastomere at the 24-cell stage(20). *nob-1* is expressed 1-2 cell cycles later, in the posterior daughters or grand-daughters of four of these *ceh-13*-expressing cells(22). In addition, both *ceh-13* and *nob-1* are expressed in the posterior daughter of the intestinal blastomere E ("Ep"). This raises the question of whether *ceh-13* regulates *nob-1* in these lineages. Expression of both factors at later stages is regulated by feedback mechanisms; early *ceh-13* activity is required for later ceh-13 expression(24), and early *nob-1* negatively regulates later *nob-1* expression through the microRNA *mir-57*(22).

Here we analyzed the *cis*-regulatory control of *ceh-13* and *nob-1* expression in the early embryo. We find that nob-1 expression is regulated by several partially redundant distal enhancers, including at least three that drive overlapping patterns during gastrulation. Two of these enhancers are positively regulated by *ceh-13*, while a third appears to be regulated by a *ceh-13*-independent mechanism. We further identified the GATA family transcription factor *elt-1*, previously known as a specifier of epidermal fate, as one of several additional positive regulators of *nob-1* expression. Detailed analysis of cell positions and cell division timing identifies both position defects and defects in cell division patterns and timing in *ceh-13* and *nob-1*/*php-3* mutants. This positive regulation of a posterior Hox gene by an anterior Hox gene suggests a novel role of Hox genes in early lineage specification.

99 # Results

100

101 **The anterior Hox gene *ceh-13* and the posterior Hox gene *nob-1* are expressed**
102 **sequentially in gastrulating embryos**

103 To better understand the expression dynamics of the *ceh-13, nob-1,* and *php-3* Hox
104 genes during embryogenesis (Figure 1), we collected 3D time-lapse movies (~1.5 minute
105 temporal resolution) of embryos expressing either *ceh-13, nob-1* or *php-3* tagged with GFP at
106 their C-termini at the endogenous locus by CRISPR/Cas9 genome editing. The same embryos
107 also expressed a ubiquitously expressed mCherry-tagged histone transgene to allow for cell
108 lineage tracing. We traced cells from soon after fertilization (4-8 cell stage) through the last
109 round of cell divisions for most cells (bean stage) by using StarryNite automated cell tracking
110 software, and quantified reporter expression in each cell across time(25–28). Note, each
111 Hox::GFP fusion line is homozygous viable, fertile, and displays no obvious phenotypes,
112 demonstrating that the fusion proteins largely function like the wild type proteins.

113

114 Consistent with previous studies using shorter reporters (20), CEH-13 expression is first
115 seen eight Wnt-signaled cells (that are the more-posterior daughter after cell division) and their
116 progeny at the 26-cell stage, during early gastrulation (Figure 1B,C, Supplemental Figure 2).
117 These include the AB lineage-derived cells ABalap, ABalpp, ABarpp, ABplap, ABplpp, ABprap
118 and ABprpp, and the posterior endoderm progenitor Ep. The ABalap and ABalpp expression
119 was barely detectable and quickly faded, while the other lineages had more robust and
120 persistent expression. . By the 200-350 cell stage, many of the granddaughters of the initially
121 expressing cells have lost CEH-13 expression, while a few cells fated to become blast cells or
122 neurons sustained or increased their expression. Also at this stage, some cells in the D and MS
123 lineages as well as a few additional AB-derived cells activate CEH-13 expression (Figure 1D).

124 We compared the reporter expression pattern to that of endogenous mRNA as measured in a
125 lineage-resolved single cell RNA-seq dataset, and found that the mRNA and reporter
126 expression patterns were consistent (29). In comparison, a rescuing 35 kb CEH-13::GFP fosmid
127 transgene had brighter expression in the cells expressing the CRISPR-tagged protein, plus
128 additional weak expression detectable in some epidermal precursors from the C lineage
129 (possibly detectable due to higher copy number). A shorter reporter containing only 8.2 kb of
130 upstream sequence lacked expression in the MS lineage, emphasizing the role of distal
131 regulatory elements in regulating *C. elegans* Hox gene expression (Supplemental Figure 1D)
132 (30,31).
133
134 Next, we defined the embryonic expression patterns of the posterior Hox genes *php-3*
135 and *nob-1* tagged with GFP at the endogenous locus. As expected, *nob-1* and *php-3,* which are
136 adjacent in the genome with *php-3* directly downstream of *nob-1*, and are expressed in identical
137 patterns in both our GFP imaging data (Supplemental Figure 1A) and in the single-cell RNA-seq
138 data (29). NOB-1/PHP-3 expression begins during mid-gastrulation in cells derived from the
139 cells ABplapp, ABplppp, ABprapp, ABprppp, Ep, and the four posterior great-granddaughters of
140 the C blastomere. Expression becomes stronger one cell cycle later in the AB-derived lineages
141 with the exception of ABp(l/r)appa. Additional late embryonic expression occurs in the
142 ABp(l/r)papppp lineages starting at the onset of morphogenesis ("bean" stage). NOB-1-
143 expressing lineages give rise to fates including neurons, hypodermis, seam cells, epithelial
144 cells, intestine, and death, and have posterior positions clustered in and near the developing tail
145 at comma stage (32). Like CEH-13, early NOB-1::GFP expression persists through the terminal
146 cell divisions in only a subset of cells (Figure 1D). A previously described NOB-1::GFP rescuing
147 transgene that includes 9kb of sequence upstream of the *nob-1* transcript expresses GFP in a
148 similar pattern, except it is not expressed in the C great-granddaughter lineages, suggesting this

149 expression requires additional regulatory sequences outside of this region (Figure 1D,
150 Supplemental Figure 1)(22).
151
152 Early CEH-13::GFP expression occurs in cells that are distributed broadly along the
153 anterior-posterior axis (Figure 1B), while NOB-1 and PHP-3 expression is more limited to the
154 posterior of the embryo. In the AB lineage, NOB-1/PHP-3 are expressed exclusively in cells that
155 were the posterior sister after cell division and whose mother expressed CEH-13 (Figure 1D-H).
156 In addition, these three genes are co-expressed at similar onset times in the posterior intestine
157 lineage derived from Ep. In contrast, in late embryos, high levels of CEH-13::GFP and NOB-
158 1::GFP/PHP-3::GFP are largely mutually exclusive (Figure 1D, Supplemental Figure 1F, G),
159 consistent with classic models of Hox expression and posterior dominance.
160
161 **Several overlapping lineage specific enhancers regulate *nob-1* embryonic expression**
162
163 To identify regulators of *nob-1* embryonic expression, we tested nearby genomic
164 sequences for embryonic *cis*-regulatory activity (Figure 2A,B). Previous work showed that other
165 *C. elegans* Hox genes are regulated by distal enhancers located as much as 20kb from a given
166 gene's promoter (24,30,33), but enhancers for *nob-1* and *php-3* have not been identified. We
167 took advantage of existing reporters of different lengths to narrow the sequence search space
168 for *nob-1* embryonic enhancers (Figure 2C). A transcriptional reporter containing just 5.3 kb of
169 upstream sequence driving histone-mCherry reporter expression, and the rescuing 9kb NOB-
170 1::GFP reporter are expressed in most of the same lineages as endogenous NOB-1::GFP,
171 indicating they contain regulatory sequences sufficient for expression in full set of expressing
172 lineages. However, while the protein fusion reporters are expressed at similar levels in each
173 lineage, the shorter 5.3kb transcriptional reporter has much lower expression in the ABp(l/r)ppp

174 lineages compared to other expressing lineages (Figure 2C, D). This suggests that additional
175 sequences between -5.3kb and -9kb are required for the full endogenous expression levels in
176 ABp(l/r)ppp.
177
178 Although other *Caenorhabditis* species have large (12-20kb) intergenic regions
179 upstream of *nob-1*, there is no detectable sequence conservation in the 5.3kb region upstream
180 of *nob-1*, and only two short conserved stretches (85 and 275 nucleotides long) between 5.3
181 and 9kb upstream (34–37). This indicates that any conserved regulatory elements in this region
182 have diverged substantially at the sequence level during *Caenorhabditis* evolution, limiting utility
183 evolutionary conservation to identify enhancers. Chromatin marks typically used to identify
184 transcriptional enhancers such as H3K27ac, H3K4me, or chromatin accessibility from whole
185 embryos did not show strong peaks near *nob-1* or near 20 additional genes expressed in
186 lineage-specific patterns at the same stage as *nob-1* (31,38–40).
187
188 We hypothesized that these chromatin signals are diminished in early embryonically
189 expressed genes because the experiments used embryos of mixed stages where later stage
190 nuclei dramatically outnumber nuclei from earlier stages. Therefore, we searched for other
191 factors with published genomic binding patterns that could mark embryonic enhancers. One
192 pattern stood out as preferentially bound near genes expressed with lineage-specific patterns in
193 the early embryo: binding of a NHR-2::GFP fusion protein (41,42). NHR-2::GFP binds in the
194 intergenic sequences upstream of 19 of these 20 genes, and 16 genes have multiple clustered
195 NHR-2 binding sites (vs. 22% and 8% of randomly chosen genes, respectively, $p < 0.001$; chi-
196 squared test). NHR-2 is a nuclear hormone receptor distantly related to mammalian thyroid and
197 PPAR receptors, and NHR-2::GFP is expressed in most or all somatic cells from the ~50-cell to
198 ~200-cell stages. The functional importance of NHR-2 binding is unclear; *nhr-2* RNAi causes

199 embryonic and larval arrest, but partial deletion alleles are viable. However, regardless of its
200 function, we hypothesized that these clustered NHR-2 binding sites might be useful proxies for
201 accessible chromatin and could predict enhancer activity in the early embryo.
202
203 We tested four NHR-2::GFP-bound regions upstream of *nob-1* for enhancer activity by
204 generating transgenic worms expressing histone-mCherry under the control of each candidate
205 enhancer placed upstream of a *pes-10* minimal promoter, which drives no consistent embryonic
206 expression on its own (Figure 2A, B). We also tested four additional sequences for which we
207 observed no NHR-2::GFP binding but which contained putative binding motifs for POP-1/TCF,
208 which is required for expression of the *nob-1* transcriptional reporter (23). We identified
209 embryonic cells expressing each enhancer reporter by confocal time lapse imaging and
210 StarryNite. Only three of the regions (-3.4kb, -4.3kb and -8.3kb) tested showed enhancer activity
211 that was consistent between embryos and also overlapped with the endogenous NOB-1::GFP
212 expression pattern, suggesting they represent functional enhancers (Figure 2C, Supplemental
213 Figure 2). All three functional enhancers were identified on the basis of NHR-2 binding.
214
215 The -3.4kb enhancer recapitulates most of the *nob-1* early embryonic expression
216 pattern, with some differences in the C lineage, and drives much weaker expression in
217 ABp(l/r)ppp than in ABp(l/r)app, similar to the *nob-1* -5.3 kb upstream transcriptional reporter.
218 The -4.3kb enhancer also drives expression in ABp(l/r)app and ABp(l/r)ppp at a very high level
219 (Figure 2D) and also variable misexpression in cells that don't normally express NOB-1 (Figure
220 2C, Supplemental Figure 2A). When this enhancer was cloned downstream of the reporter, it
221 showed less ectopic expression and stronger expression in ABp(l/r)app relative to ABp(l/r)ppp,
222 similar to the -3.4 kb enhancer. This confirms the -4.3kb region as a *bona fide* enhancer capable
223 of acting at a distance and suggests that the placement of this enhancer relative to the promoter

influences its activity differently in different lineages and may be important for specificity. Embryos carrying multiple copies of the -4.3kb reporter transgene occasionally displayed the "no backend" phenotype observed in *nob-1/php-3* mutant embryos (Supplemental Figure 2B) (5). A third *nob-1* enhancer (-8.3kb) drives early embryonic expression only in ABp(l/r)ppp, as well as later expression in ABp(l/r)papppp. This most-distal enhancer is included in -9kb NOB-1::GFP transgene but not the shorter -5.3kb transcriptional reporter, and includes the only substantial stretch of conserved sequence in the *nob-1* promoter region. This region thus can explain why ABp(l/r)ppp expression is relatively stronger in the translational reporter compared to the shorter transcriptional reporter.

As the -5.3kb *nob-1* transcriptional reporter includes both the -3.4kb and -4.3kb enhancers, we deleted each enhancer from this construct to test their necessity for *nob-1* expression (Figure 2C). Deleting both enhancers led to a complete loss of early embryonic expression in both AB lineages, suggesting there are no additional enhancers present sufficient for early embryonic expression in these lineages. The deletion of the -3.4 kb enhancer did not disrupt expression in ABp(l/r)app, ABp(l/r)ppp and in the absence of the -4.3 kb enhancer, this enhancer was not sufficient to rescue expression in these lineages. This indicates that while the -3.4kb enhancer may be sufficient to drive expression when placed directly next to the promoter, it is unable to drive expression in the endogenous context. Conversely, the -4.3 kb enhancer is a key driver of expression in these lineages. The expression remaining when both enhancers are lost indicates that additional sequences that drive the expression in the Ep and Cpapp lineages must exist within the -5.3 kb upstream region.

249 ***ceh-13* and Hox cofactors activate *nob-1* expression**

250 Because *ceh-13* expression precedes that of *nob-1* in many lineages, we asked whether
251 *ceh-13* is required for *nob-1* expression. To evaluate this, we examined *nob-1* reporter
252 expression in embryos homozygous for the likely null mutation *ceh-13(sw1)* (21). Expression of
253 the -5.3kb *nob-1* transcriptional reporter is eliminated in ABp(l/r)ppp ($p < 0.001$), and decreased
254 by 25% in ABp(l/r)ap, and 40% in Ep ($p < 0.02$) (Figure 3A-C). Depletion of *ceh-13* by RNAi
255 gave similar results with the transcriptional reporter ($p < 0.002$). In contrast, *ceh-13* RNAi does
256 not significantly alter expression of the -9kb NOB-1::GFP transgene, indicating that there are
257 additional cis-regulatory elements in this reporter which are *ceh-13* independent (Supplemental
258 Figure 3A).

259

260 To determine which enhancers require *ceh-13*, we measured the activity of individual
261 *nob-1* enhancer reporters in worms lacking *ceh-13* (Figure 3A, Supplemental Figure 3A). In *ceh-*
262 *13* mutants, expression driven by the -3.4 kb enhancer decreased significantly in all expressing
263 cells, excluding the C lineage ($p < 0.003$) with an average decrease of 90% and complete loss
264 in ABp(l/r)ppp. *ceh-13* loss also reduces activity of the -4.3 kb enhancer in ABp(l/r)ppp (47%
265 decrease) but expression in ABp(l/r)ap is unchanged. This indicates that other factors besides
266 *ceh-13* activate this enhancer in ABp(l/r)ap and suggests that this enhancer may be responsible
267 for the residual expression of the 5.3kb transcriptional regulation in this lineage in *ceh-13*
268 mutants. The distal -8.3kb enhancer also lost expression in ABp(l/r)ppp in the ceh-13(sw1)
269 mutant ($p < 0.002$), indicating its activity also requires *ceh-13*. Motif analysis identified six
270 putative *ceh-13*-binding motifs in the -3.4kb enhancer; mutating these sites abolished
271 expression in the AB and C lineage ($p < 0.02$, $p < 0.03$), but did not alter expression in the Ep
272 lineage indicating *ceh-13* regulation of *nob-1* may be indirect in the E lineage (Figure 3A,
273 Supplemental Figure 3B). These results show that multiple *ceh-13*-dependent enhancers work
274 together to regulate *nob-1* expression in gastrulating embryos.

275

276 Expression of classically defined Hox targets often require Hox cofactors such as
277 *homothorax* or *extradenticle*. These cofactors form larger TF complexes with Hox factors to
278 increase binding specificity and may also have Hox-independent functions (43–45). To
279 determine when and where Hox cofactors are expressed in early embryos, we used StarryNite
280 to trace the expression of translational reporters for *unc-62*, the *C. elegans homothorax/Meis*
281 homolog, and of *ceh-20* and *ceh-40*, the homologs of *extradenticle/Pbx*. A third *extradenticle*
282 homolog, *ceh-60*, is only expressed in later development (>200 minutes) and does not overlap
283 with *ceh-13*, so was not investigated further(29). We found that each of these genes has
284 specific and dynamic expression patterns that overlap with each other and with *ceh-13* and *nob-*
285 *1* expression (Figure 4A-D, Supplemental Figure 5). In particular, all three cofactors are
286 coexpressed with CEH-13 in cells that will later express NOB-1. Other CEH-13 and NOB-1
287 expressing cells also express all three cofactors, except only CEH-20 is expressed in the early
288 E lineage, and all three are lost in the NOB-1-expressing ABp(l/r)appp lineage as the embryo
289 approaches morphogenesis. We conclude that Hox cofactors are expressed in cells where *ceh-*
290 *13* activates *nob-1* expression.

291

292 We tested whether Hox cofactors regulate *nob-1* expression by examining *nob-1*
293 reporter expression after loss of each gene. We found that depleting *unc-62* by RNAi led to
294 significant loss of expression of the *nob-1* -5.3kb reporter in all AB lineages (80% decrease,
295 p=0.001), with near complete loss in the ABp(l/r)apap and ABp(l/r)ppp lineages (Figure 4E). The
296 -9kb NOB-1:GFP protein reporter showed similar expression decreases, although this was only
297 significant in ABp(l/r)appa and incompletely penetrant in other lineages (Supplemental Figure
298 4B-C). In contrast, CEH-13::GFP reporter expression was unchanged after *unc-62*
299 RNAi (Supplemental Figure 4D). These results show that *nob-1* is regulated by *unc-62*. The

300 fact that *unc-62* RNAi has a stronger phenotype in ABp(l/r)appa than loss of *ceh-13* suggests
301 that *unc-62* may regulate *nob-1* independently of *ceh-13* in these cells.
302
303 To investigate the role of the *extradenticle* homologs, we examined the *nob-1*
304 transcriptional reporter in a *ceh-40(gk159)* null mutant background in embryos of worms treated
305 with control or *ceh-20* RNAi. We found that the combination of *ceh-20* RNAi with the *ceh-40*
306 mutation caused a significant loss of expression in virtually all expressing cells including Ep and
307 Cpap as compared to control RNAi (97% decrease, $p < 0.004$). This indicates that the *exd*
308 homologs *ceh-20* and *ceh-40* are required to activate *nob-1* expression and that they are at
309 least partially independent of *ceh-13* in the ABp(l/r)ap, Ep, and Cpap sublineages. This finding is
310 consistent with previous reports that *nob-1* RNAi causes increased lethality in a *ceh-40* mutant
311 background relative to wildtype animals (46).
312
313 **Multiple lineage-specific embryonic TFs including *elt-1/GATA*, *ceh-36/OTX* and *unc-***
314 ***30/PITX* are required for early *nob-1* expression**
315 Since some NOB-1::GFP reporter expression remains in the absence of *ceh-13*,
316 especially in the ABp(l/r)ap lineage, other factors must also activate *nob-1* in these cells.
317 Indeed, we previously identified the Wnt effectors *pop-1* and *sys-1* as activators of *nob-1*
318 expression (23). We took advantage of databases of TF expression to search for additional
319 candidate regulators (29,40,47).
320
321 Only two of the three enhancers (-3.4kb and -4.3kb) drive expression in the ABp(l/r)ap
322 lineage, so to identify additional potential regulators of *nob-1* in this lineage, we used two
323 criteria. First, we searched for TFs expressed specifically in ABp(l/r)ap, but not ABp(l/r)pp.
324 Second, we used a TF binding site scanning approach to identify which of these TFs have

325 predicted binding motifs in the -3.4kb and -4.3kb enhancers (9,48). From this analysis, the
326 GATA zinc finger encoded by *elt-1* emerged as the strongest candidate. An ELT-1::GFP
327 reporter is expressed prior to gastrulation in the ABp(l/r)ap progenitors ABpla and ABpra, in the
328 other major epidermis-producing lineages ABarp, Caa and Cpa, and in the primarily neuronal
329 lineages ABalap and ABalppp (Figure 5A). ELT-1::GFP expression is later downregulated in
330 cells that do not adopt epidermal fates (Figure 5B). ELT-1::GFP expression in the ABpla/ABpra
331 lineages could be detected at least 20 minutes prior to *nob-1* reporter expression in ABp(l/r)ap
332 (Figure 5B, C). GATA Motifs predicted to bind ELT-1 are enriched in the ABp(l/r)ap enhancers -
333 3.4kb (8 sites) and -4.3kb (7 sites) enhancers compared to the -8.3 enhancer (1 site), which
334 does not drive expression in ABp(l/r)ap. While the *C. elegans* genome encodes several other
335 GATA factors, only *elt-1* is expressed prior to *nob-1* in the ABp(l/r)a linage(29,49).
336
337 To test whether *elt-1* regulates *nob-1* expression, we measured the activity of *nob-1*
338 reporters in the *elt-1(ok1002)* null mutant background (Figure 5E-G, Supplemental Figure 6A,B).
339 We found that *elt-1* mutants showed decreased expression of the *nob-1* transcriptional reporter
340 in the ABp(l/r)ap lineage (87% decrease, $p < 0.014$), and the Cpap lineage (92% decrease, not
341 significant), in which *elt-1* precedes *nob-1* expression, but not in ABp(l/r)pp, where ELT-1::GFP
342 is not expressed. Similarly, we observed decreases in the same sublineages for the -3.4kb
343 enhancer reporter (ABp(l/r)ap: 72% decrease, $p < 0.008$; C: 71% decrease, $p < 0.03$) and the -
344 4.3kb enhancer reporter (ABp(l/r)ap: 31% decrease, not significant). To determine if *elt-1*
345 directly regulates the -3.4kb enhancer, we mutated the predicted ELT-1 binding sites, which
346 have a characteristic GATA motif, and observed loss of reporter expression in all lineages ($p <$
347 0.001). We conclude that *elt-1* activates *nob-1* expression in the ABp(l/r)ap lineage through at
348 least two enhancers, and is at least partially redundant with other factors that may bind GATA
349 motifs.

350

351 We previously showed that two homeodomain *bicoid* family TFs, *ceh-36/OTX* and *unc-*
352 *30/PITX* are redundantly required for proper development of the ABp(l/r)p lineage (50). Since
353 *ceh-13* and *elt-1* mutants still have some *nob-1* reporter expression in the ABp(l/r)p
354 descendants, we hypothesized that *ceh-36* and *unc-30* might be important for *nob-1* expression
355 in these lineages. All three enhancers contain at least two putative CEH-36/UNC-30 binding
356 sites, and the -8.3 kb enhancer, which activates expression only in ABp(l/r)p, has nine
357 (Supplemental Tables S3-S5). To test this hypothesis, we examined NOB-1::GFP transgene
358 expression in eight *ceh-36;unc-30* double mutant embryos, and found that two of the eight
359 embryos (25%) lost expression in this lineage (Supplemental Figure 7A). Furthermore, the ratio
360 of ABp(l/r)ap to ABp(l/r)ppp expression significantly increased ($p < 0.002$) in the remaining
361 double mutant embryos, consistent with a decrease in ABp(l/r)ppp expression (Supplemental
362 Figure 7B). In conclusion, at least seven partially redundant lineage-specific transcription factors
363 positively regulate *nob-1* expression: *ceh-13, ceh-20, ceh-40, unc-62, elt-1*, *ceh-36,* and *unc-30*.
364

365 ***ceh-13 and nob-1 are required for correct cell position and division patterns in the early***
366 ***embryo***

367 Previous work suggested that *nob-1/php-3* and *ceh-13* are required for cell position but
368 not other aspects of cell fate specification (5). However, mutating lineage identity regulators
369 often leads to defects in cell cycle length or division patterns (50,51) that could have been
370 missed in previous studies. To test for such defects, we measured cell positions and cell
371 division timing in six *nob-1/php-3* (referred to as nob-1 for simplicity) and *ceh-13* mutant
372 embryos by time-lapse microscopy and StarryNite cell tracking, and compared them to a
373 database of 17 wild type embryos (27,50). (Figure 6)
374

375 Consistent with previous work (5), we observed striking global patterns of cell position
376 defects in *nob-1* mutant embryos. The most severe and highest penetrance defects were in
377 cells from NOB-1-expressing lineages (Figure 6A,C,D,G, Supplemental Figure 8)). In total, 48%
378 (62 of 127) of cells descended from NOB-1::GFP expressing lineages had severe position
379 defects (>5 micron deviation, z score > 3.5) in at least two embryos compared to 1.2% (14 of
380 1094) of cells from non-expressing lineages ($p << 10^{-20}$). However, a large number of cells from
381 non-expressing lineages were moderately mis-positioned, suggesting that many defects are not
382 cell-autonomous. Globally, dorsal cells that normally express NOB-1 fail to migrate to the
383 posterior at 230 minutes post-fertilization; by 300 minutes non-expressing ventral cells
384 compensate by inappropriately moving to the posterior, resulting in a global counterclockwise
385 rotation of cell positions when the embryo is viewed from the left aspect (Figure 6G). The
386 position defects we observed are consistent with the severe posterior morphology defects
387 observed in rare surviving larvae.
388
389 We also identified broad cell position defects in *ceh-13* mutant embryos (Figure
390 6B,E,F,H,I). Intriguingly, the global patterns of cell position defects differed from *nob-1* mutants.
391 The number of severe position defects was lower for *ceh-13* than for *nob-1*, with 4% (15/357) of
392 cells descended from CEH-13::GFP expressing lineages severely displaced in at least two
393 embryos, as opposed to 0.5% (5/874) of cells from non-expressing lineages ($p << 10^{-20}$). At 210
394 minutes, (200 cell stage), the most strongly mispositioned cells were *ceh-13*-expressing cells
395 that do not express *nob-1* in the posterior ventral region of the embryo. At this stage, cells on
396 the dorsal surface were posteriorly mispositioned, such that cells in the posterior half of the
397 embryo were rotationally mispositioned clockwise, the opposite direction to that seen in *nob-1*
398 mutants (Figure 6H). Cells at the anterior ventral surface (both *ceh-13*-expressing and non-
399 expressing) were mispositioned towards the posterior, resulting in a counterclockwise rotational
400 defect in the anterior half of the embryo. At later stages, these global defects were largely

401 resolved, and after the onset of morphogenesis the position defects were largely limited to a
402 small number of strongly mispositioned cells (Figure 6I). The most extreme were the DA and
403 SAB motorneurons after 300 minutes (bean stage), which were mispositioned several cell
404 diameters anterior of their wild-type position (Supplemental Figure 8B). Given the recovery of
405 most cell positions by the beginning of morphogenesis, it is unclear if cell position defects
406 contribute to the severe anterior morphogenesis phenotypes in *ceh-13* mutants that hatch (21),
407 although the earlier cell position defects could disrupt normal cell-cell signaling interactions
408 required for fate specification.
409
410 In contrast to previous studies (5,21), we also identified numerous defects in cell division
411 timing or pattern in both *nob-1* and *ceh-13* mutants, and these were also heavily restricted to
412 expressing lineages (Figure 6A,B). 13% of *nob-1* expressing cells and 5% of *ceh-13* expressing
413 cells had severe division-time defects in at least two of the corresponding mutant embryos (>5
414 minute deviation from wild type, and z-score >5), vs none in non-expressing cells ($p << 10^{-20}$).
415 The most common cell division defect in *nob-1* mutants was the PLM/ALN neuroblast mother
416 (ABp(l/r)apappp), which failed to divide in 8 of 12 observations (Figure 6J). The neuroblast that
417 normally produces the PHA, PVC and LUA neurons instead underwent programmed cell death
418 in two of 12 mutant lineages. Other cells that had multiple cell cycle delays in *nob-1* mutants
419 included the PVQ neuroblast, PHB/HSN neuroblast, and the mother of the epidermal cells
420 PHsh, hyp8 and hyp9. All of these cells also were mispositioned (mean 5 micron deviation from
421 expected position, Supplemental Figure 8C).
422
423 The most striking defects in *ceh-13* mutants were in the cells ABarppaaa(a/p), which
424 normally differentiate into the ADE sheath (glial) cell and H2 epidermal cell, but instead each
425 divided inappropriately in 4 of 6 mutant embryos (Figure 6K). In addition, ABplppaaap, which
426 normally undergoes programmed cell death, instead divided in two *ceh-13* mutant embryos.

427 Several neuroblasts including those producing the DA, DD and SAB motorneurons also had cell
428 division delays in *ceh-13* mutants. We conclude that both *ceh-13* and *nob-1/php-3* are required
429 not only for proper cell positioning, but also for normal division patterns, suggesting a broader
430 role in fate specification. Furthermore, the incomplete penetrance of both cell cycle and cell
431 position defects in *ceh-13* and *nob-1* mutants indicate redundancy in developmental
432 programming that likely contributes to the robustness of *C. elegans* embryonic development
433 (Sulston, 1983).
434

435 ## Discussion

436

437 Classic work defined the concept of Posterior Dominance, in which posterior Hox genes
438 repress the expression and activity of more anterior Hox genes (1). Indeed, previous work in
439 later developmental stages showed that *nob-1* represses *ceh-13* in the posterior ventral nerve
440 cord, consistent with posterior dominance (45). In contrast, we show that *ceh-13* activates *nob-*
441 *1/php-3* expression through at least two enhancers during *C. elegans* gastrulation. To our
442 knowledge, this is the first example of an anterior Hox gene positively regulating the expression
443 of a posterior Hox gene during development. *ceh-13* and *nob-1/php-3* are also expressed at an
444 earlier phase in development (pre-gastrulation for *ceh-13* and mid-gastrulation for *nob-1/php-3*)
445 than in many other organisms. These observations, along with the lineage defects seen in *ceh-*
446 *13* and *nob-1* mutants, suggest that the role of *ceh-13* and *nob-1* is to regulate lineage identity,
447 distinct from their later role in positional identity. The role of Hox cofactors such as *unc-62, ceh-*
448 *20* and *ceh-40* in early embryonic *nob-1* regulation suggests that these novel functions in
449 lineage specification nonetheless share some common mechanisms with the later roles. The
450 fact that *C. elegans* is largely unsegmented may have allowed the cooption of these Hox genes

451 for this distinct role. This emphasizes the striking amount of flexibility in the *C. elegans* Hox
452 cluster.
453
454 Several studies have highlighted that conserved transcription factors often "moonlight,"
455 with the same factor playing apparently distinct roles in early progenitors and in terminal cell
456 types. For example, the OTX homeodomain TF *ceh-36*, and the PITX homeodomain TF *unc-30*,
457 which both specify specific terminal neuron types, separately act redundantly 6-7 cell divisions
458 earlier in the ABp(l/r)p lineages to specify broad features of lineage identity (50,52–54), and *skn-*
459 *1*, which is required maternally to specify the endomesodermal blastomere EMS at the 4-cell
460 stage is required postembryonically for oxidative stress resistance and longevity (55,56). Our
461 work shows that *ceh-13* and *nob-1/php-3* are another example of this phenomenon. Our
462 identification of cell division defects in each mutant demonstrates they also play a role in lineage
463 specification. In addition, we confirmed that each is also required for correct cell position; it is
464 important to note that position defects could also result from incorrect specification of lineage
465 identity. Previous work showed that at least one neuron (the PLM touch receptor) is defective in
466 less severe *nob-1* mutants(19); the failure of PLM neuroblasts to divide in *nob-1/php-3* mutants
467 indicates a function in PLM progenitor lineages. Similarly, *ceh-13* mutants have cell division
468 defects, and *ceh-13* is required for the lineage-specific activity of specific *nob-1* enhancers.
469 Finally, while *elt-1* has a well-defined known role in epidermal fate specification(57), our work
470 shows that it is also required for *nob-1* enhancer activity. This is consistent with other recent
471 work identifying defects in cell division patterns and the expression of the neurogenic TF *lin-32*
472 in *elt-1* mutants(58). The ability of developmental transcription factors to "moonlight' is likely
473 facilitated by complex regulation by multiple enhancers as seen for *nob-1/php-3*, and *ceh-*
474 *13*(30,31) since enhancer evolution can enable genes to be expressed at different locations and
475 times in development(59,60). An intriguing question is whether these multiple Hox functions are

476 made possible by the unique nature of the *C. elegans* lineage, where positional identity is
477 defined at least in part by lineage history (17,61), or if they are conserved in other species.
478
479 While early reporter studies found that the expression of many genes expressed in
480 terminal cells is well approximated using just the promoter-proximal region(62–64), open
481 chromatin mapping studies have identified many distal regions of open chromatin, many of
482 which can act as enhancers (31,38,39). Our work reinforces these studies and emphasizes the
483 importance of enhancers in *C. elegans* gene regulation. Intriguingly, other genes expressed in
484 lineage-specific patterns around the same time as *nob-1* have similar tendency to have multiple
485 nearby regions of NHR-2::GFP binding and lineage-specific accessible chromatin as measured
486 by ATAC-seq (65), suggesting they may also be regulated by multiple distal enhancers. This
487 could reflect these genes' need for more complex regulation. The *nob-1/php-3* locus contains at
488 least two or three enhancers responsible for expression in each expression domain during
489 gastrulation. This is reminiscent of so-called "shadow enhancers" identified in other organisms,
490 for which redundancy appears to confer robustness in the face of environmental variability(66–
491 68). This high level of redundancy also appears to extend to the number of transcription factors
492 regulating each enhancer. Current data implicate at least eight TFs as activators of *nob-1*
493 enhancers including *ceh-13*, *elt-1*, *ceh-36*, *unc-30*, the Wnt effector *pop-1*, and the Hox co-
494 factors *ceh-20*, *ceh-40* and *unc-62* (Supplemental Figure 9). In some cases, the same binding
495 motif may be regulated by different factors in different lineages. For example, mutating six
496 GATA motifs in the -3.4 kb enhancer caused the loss of expression in ABp(l/r)ap, potentially due
497 to loss of ELT-1 binding. However, this mutant also lost expression in Ep, which does not
498 express *elt-1*, but does express other GATA factors with similar binding specificity including
499 *end-1*, *end-3*,and *elt-7* (69). Similarly, the more severe loss of *nob-1* enhancer expression when
500 CEH-13 motifs are mutated than observed in *ceh-13* mutant animals indicates that other TFs
501 may also bind these sites. The partially penetrant nature of many of the mutant phenotypes

502 further emphasizes the high level of redundancy. In sum, multiple modes of regulatory
503 redundancy could provide a mechanism for the remarkable developmental robustness observed
504 in *C. elegans.*
505

506 ## Methods

507

508 Strain generation and propagation

509 Worm strains (Supplemental Table 1) were maintained at 21-23°C on OP50 *E. coli* on NGM
510 plates. Enhancer reporter strains were generated by injection into RW10029, a GFP histone
511 strain used for lineage tracing. Injection cocktails consisted of reporter DNA construct at
512 10ng/μL, with 5 ng/μL myo-2p::GFP and 135 ng/μL pBluescript vector and were injected using a
513 Narishige MN-151 micromanipulator with Tritech microinjector system. The *nob-1* promoter
514 deletion strains were generated by injection and compared to a wildt-ype *nob-1* promoter strain
515 created by injection of pJIM20::nob-1, JIM518. The *ceh-13* rescuing fosmid, *ujIs153*, was
516 created by bombardment of WRM0622C_C06 (70) as previously described (50). Other strains
517 were created through crosses using standard approaches. Lethal alleles were maintained as
518 balanced heterozygotes (*ceh-13(sw1))* or rescued by free duplications (*nob-1(ct223)*), with
519 homozygous mutants recognized by characteristic high-penetrance morphology defects. Note,
520 the *ct223* allele disrupts both *nob-1* and *php-3*. Lethal *ceh-36;unc-30* double mutants were
521 maintained as homozygotes rescued by an extra-chromosomal array carrying *ceh-36*::GFP; lack
522 of rescue was scored by absence of GFP in the ABpxpa lineage. CEH-13::GFP and NOB-
523 1::GFP CRISPR knock-in alleles were created under contract by SUNY Biotech (Fuzhou,
524 China).
525

526 Molecular biology

527 Candidate enhancers were amplified with Phusion HF polymerase (New England Biosciences)
528 from either pJIM20::nob-1 or N2 genomic DNA, with overhangs for stitching, which were then
529 either gel or PCR purified (Qiagen). Putative enhancers were attached to a *pes-10* minimal
530 promoter::HIS-24::mCherry::let-858 3'UTR fragment amplified from POPTOP plasmid (71)
531 (Addgene #34848) by using PCR stitching to create an enhancer reporter which was sequence
532 verified and purified with a PureLink PCR purification kit (ThermoFisher) for injection. The *pes-*
533 *10* minimal promoter drives no consistent early embryonic expression alone, but has previously
534 been shown to facilitate expression driven by different enhancers (71–73). For the downstream
535 enhancer experiment, the -4.3kb enhancer was cloned immediately downstream of the reporter
536 stop codon. Tested enhancer sequences can be found in Supplemental Table 2. Regions
537 deleted from the -5.3 kb transcriptional reporter match the tested enhancer sequences exactly.
538 Putative transcription factor binding sites were identified using CIS-BP
539 (cisbp.ccbr.utoronto.ca)(9,48) (Supplemental Table 3-5). DNA fragments with desired mutations
540 were synthesized (Integrated DNA Technologies) and PCR stitched as before.
541
542 Imaging/Lineaging
543 We acquired confocal images with a Leica TCS SP5, Stellaris or Nikon A1RSi resonance
544 scanning confocal microscope (67 z planes at 0.5 µm spacing and 1.5 minute time spacing, with
545 laser power increasing by 4-fold through the embryo depth to account for attenuation of signal
546 with depth). Embryos from self-fertilized hermaphrodites were mounted in egg buffer/methyl
547 cellulose with 20µm beads as spacers (74) and imaged at 22°C using a stage temperature
548 controller (Brook Industries, Lake Villa, IL). We used StarryNite software to automatically
549 annotate nuclei and trace lineages, and AceTree software to identify and fix any errors from the
550 automated analysis, and quantified reporter expression in each nucleus relative to local
551 background (using the "blot" background correction technique) as previously described
552 (25,26,28,75,76).

553

554 Quantitative comparisons

555 Cell averages of nuclear fluorescence were computed for each cell based on all (typically >20)
556 measurements across its lifetime (Supplemental Table 6). For each control condition, the mean
557 control value of each named expressing cell was computed and used to determine the fold
558 change for each control and mutant cell with the same name, which were displayed as boxplots
559 using R 3.5.1 (The R Foundation for Statistical Computing). Background-corrected expression
560 values were rounded up to zero if values fell below zero. To determine if changes were
561 significant across the lineage, the summed expression for each cell in the lineage of interest
562 was calculated for all control and mutant embryos and the two sets of values were compared
563 using a Wilcoxon Ranked Sum test using R. For each condition, at least four control and three
564 mutant embryos were analyzed (exact numbers in Supplemental Table 7). Each embryo
565 analyzed represents an independent biological replicate. To evaluate the enrichment of NHR-2
566 binding sites, a chi-squared test was used.

567

568 Mutant cell position analysis

569 Cell position defects were identified as previously (50). Briefly, we corrected for differences in
570 global division rates (which did not differ dramatically from wild-type), and considered divisions
571 as defective/outliers if they deviated from the wild-type cell cycle length by at least five minutes
572 and had a z-score greater than three (Supplemental Tables 8-10). Cell positions (Supplemental
573 Tables 11-13) were corrected for differences in embryo size and rotation, and considered
574 defective if they deviated from the expected wildtype position by at least five microns, had a z-
575 score greater than five, and a nearest neighbor score greater than 0.8 (defined empirically
576 based on the distribution of wild-type scores).

Acknowledgements

We thank Brian Gebelein and members of the Murray, Zacharias, and Gebelein laboratories and the Philly Worm Group for helpful discussion and comments on the manuscript. We thank Bob Waterston and Adrian Streit for strains. Some strains were provided by the CGC, which is funded by NIH Office of Research Infrastructure Programs (P40 OD010440). We thank WormBase, which is supported by NHGRI grant U24 HG002223, for consolidating valuable information. We thank Swati Mundre, Tom Sesterhenn,Yannis Belloucif, Ilona Jileaeva for cloning assistance and technical assistance with lineage tracing and worm genetics. We thank Meera Sundaram for the use of injection equipment and reagents. We thank Stephen Nehrbass for software assistance and Matt Kofron and Evan Meyer at the Confocal Imaging Core at Cincinnati Children's, a Nikon Center of Excellence, for their help with imaging, and Matt Batie for designing and building the cooling stage. This work was supported by NIH grants R35GM127093 (to J.I.M.), R00GM111825 (to A.L.Z.), and F31GM123737 (to J.D.R.).

595 ## References Cited

596 1. Duboule D, Morata G. Colinearity and functional hierarchy among genes of the homeotic
597 complexes. Trends Genet TIG. 1994 Oct;10(10):358–64.

598 2. Noordermeer D, Duboule D. Chromatin architectures and Hox gene collinearity. Curr Top
599 Dev Biol. 2013;104:113–48.

600 3. Gaunt SJ. Hox cluster genes and collinearities throughout the tree of animal life. Int J Dev
601 Biol. 2018;62(11–12):673–83.

602 4. Bürglin TR, Ruvkun G, Coulson A, Hawkins NC, McGhee JD, Schaller D, et al. Nematode
603 homeobox cluster. Nature. 1991 Jun 27;351(6329):703.

604 5. Van Auken K, Weaver DC, Edgar LG, Wood WB. Caenorhabditis elegans embryonic axial
605 patterning requires two recently discovered posterior-group Hox genes. Proc Natl Acad Sci
606 U S A. 2000 Apr 25;97(9):4499–503.

607 6. Aboobaker A, Blaxter M. Hox gene evolution in nematodes: novelty conserved. Curr Opin
608 Genet Dev. 2003 Dec;13(6):593–8.

609 7. Schaller D, Wittmann C, Spicher A, Müller F, Tobler H. Cloning and analysis of three new
610 homeobox genes from the nematode Caenorhabditis elegans. Nucleic Acids Res. 1990 Apr
611 25;18(8):2033–6.

612 8. Bürglin TR, Ruvkun G. The Caenorhabditis elegans homeobox gene cluster. Curr Opin
613 Genet Dev. 1993 Aug;3(4):615–20.

614 9. Weirauch MT, Yang A, Albu M, Cote AG, Montenegro-Montero A, Drewe P, et al.
615 Determination and inference of eukaryotic transcription factor sequence specificity. Cell.
616 2014 Sep 11;158(6):1431–43.

617 10. Ferreira HB, Zhang Y, Zhao C, Emmons SW. Patterning of Caenorhabditis elegans posterior
618 structures by the Abdominal-B homolog, egl-5. Dev Biol. 1999 Mar 1;207(1):215–28.

619 11. Harris J, Honigberg L, Robinson N, Kenyon C. Neuronal cell migration in C. elegans:
620 regulation of Hox gene expression and cell position. Dev Camb Engl. 1996
621 Oct;122(10):3117–31.

622 12. Josephson MP, Chai Y, Ou G, Lundquist EA. EGL-20/Wnt and MAB-5/Hox Act Sequentially
623 to Inhibit Anterior Migration of Neuroblasts in C. elegans. PloS One. 2016;11(2):e0148658.

624 13. Maloof JN, Whangbo J, Harris JM, Jongeward GD, Kenyon C. A Wnt signaling pathway
625 controls hox gene expression and neuroblast migration in C. elegans. Dev Camb Engl. 1999
626 Jan;126(1):37–49.

627 14. Shemer G, Podbilewicz B. LIN-39/Hox triggers cell division and represses EFF-1/fusogen-
628 dependent vulval cell fusion. Genes Dev. 2002 Dec 15;16(24):3136–41.

629 15. Takács-Vellai K, Vellai T, Chen EB, Zhang Y, Guerry F, Stern MJ, et al. Transcriptional control
630 of Notch signaling by a HOX and a PBX/EXD protein during vulval development in C.
631 elegans. Dev Biol. 2007 Feb 15;302(2):661–9.

632 16. Tihanyi B, Vellai T, Regos A, Ari E, Müller F, Takács-Vellai K. The C. elegans Hox gene ceh-13
633 regulates cell migration and fusion in a non-colinear way. Implications for the early
634 evolution of Hox clusters. BMC Dev Biol. 2010 Jul 28;10:78.

635 17. Wang BB, Müller-Immergluck MM, Austin J, Robinson NT, Chisholm A, Kenyon C. A
636 homeotic gene cluster patterns the anteroposterior body axis of C. elegans. Cell. 1993 Jul
637 16;74(1):29–42.

638 18. Yu H, Seah A, Sternberg PW. Re-programming of C. elegans male epidermal precursor
639 fates by Wnt, Hox, and LIN-12/Notch activities. Dev Biol. 2010 Sep 1;345(1):1–11.

640 19. Zheng C, Jin FQ, Chalfie M. Hox Proteins Act as Transcriptional Guarantors to Ensure
641 Terminal Differentiation. Cell Rep. 2015 Nov 17;13(7):1343–52.

642 20. Wittmann C, Bossinger O, Goldstein B, Fleischmann M, Kohler R, Brunschwig K, et al. The
643 expression of the C. elegans labial-like Hox gene ceh-13 during early embryogenesis relies
644 on cell fate and on anteroposterior cell polarity. Dev Camb Engl. 1997 Nov;124(21):4193–
645 200.

646 21. Brunschwig K, Wittmann C, Schnabel R, Bürglin TR, Tobler H, Müller F. Anterior
647 organization of the Caenorhabditis elegans embryo by the labial-like Hox gene ceh-13. Dev
648 Camb Engl. 1999 Apr;126(7):1537–46.

649 22. Zhao Z, Boyle TJ, Liu Z, Murray JI, Wood WB, Waterston RH. A negative regulatory loop
650 between microRNA and Hox gene controls posterior identities in Caenorhabditis elegans.
651 PLoS Genet. 2010 Sep 2;6(9):e1001089.

652 23. Zacharias AL, Walton T, Preston E, Murray JI. Quantitative Differences in Nuclear β-catenin
653 and TCF Pattern Embryonic Cells in C. elegans. PLoS Genet. 2015 Oct;11(10):e1005585.

654 24. Streit A, Kohler R, Marty T, Belfiore M, Takacs-Vellai K, Vigano M-A, et al. Conserved
655 regulation of the caenorhabditis elegans labial/Hox1 gene ceh-13. Dev Biol.
656 2002;242(2):96–108.

657 25. Murray JI, Bao Z, Boyle TJ, Waterston RH. The lineaging of fluorescently-labeled
658 Caenorhabditis elegans embryos with StarryNite and AceTree. Nat Protoc. 2006
659 Nov;1(3):1468–76.

660 26. Bao Z, Murray JI, Boyle TJ, Ooi S-L, Sandel MJ, Waterston RH. Automated cell lineage
661 tracing in Caenorhabditis elegans. Proc Natl Acad Sci. 2006 Feb;103(8):2707–12.

662 27. Richards JL, Zacharias AL, Walton T, Burdick JT, Murray JI. A quantitative model of normal
663 Caenorhabditis elegans embryogenesis and its disruption after stress. Dev Biol. 2013 Feb
664 1;374(1):12–23.

665 28. Santella A, Du Z, Bao Z. A semi-local neighborhood-based framework for probabilistic cell
666 lineage tracing. BMC Bioinformatics. 2014 Jun 25;15:217.

667 29. Packer JS, Zhu Q, Huynh C, Sivaramakrishnan P, Preston E, Dueck H, et al. A lineage-
668 resolved molecular atlas of C. elegans embryogenesis at single-cell resolution. Science.
669 2019 20;365(6459).

670 30. Kuntz SG, Schwarz EM, DeModena JA, De Buysscher T, Trout D, Shizuya H, et al.
671 Multigenome DNA sequence conservation identifies Hox cis-regulatory elements. Genome
672 Res. 2008 Dec;18(12):1955–68.

673 31. Ho MCW, Quintero-Cadena P, Sternberg PW. Genome-wide discovery of active regulatory
674 elements and transcription factor footprints in Caenorhabditis elegans using DNase-seq.
675 Genome Res. 2017 Dec;27(12):2108–19.

676 32. Sulston J. The embryonic cell lineage of the nematode Caenorhabditis elegans. Dev Biol.
677 1983 Nov;100(1):64–119.

678 33. Teng Y, Girard L, Ferreira HB, Sternberg PW, Emmons SW. Dissection of cis-regulatory
679 elements in the C. elegans Hox gene egl-5 promoter. Dev Biol. 2004 Dec 15;276(2):476–92.

680 34. Coghlan A, Fiedler TJ, McKay SJ, Flicek P, Harris TW, Blasiar D, et al. nGASP--the nematode
681 genome annotation assessment project. BMC Bioinformatics. 2008 Dec 19;9:549.

682 35. Gupta BP, Sternberg PW. The draft genome sequence of the nematode Caenorhabditis
683 briggsae, a companion to C. elegans. Genome Biol. 2003;4(12):238.

684 36. Hillier LW, Miller RD, Baird SE, Chinwalla A, Fulton LA, Koboldt DC, et al. Comparison of C.
685 elegans and C. briggsae Genome Sequences Reveals Extensive Conservation of
686 Chromosome Organization and Synteny. PLOS Biol. 2007 Jul 3;5(7):e167.

687 37. Sternberg PW, Waterston RH, Spieth J, Eddy S, Wilson RK. Genome Sequence of Additional
688 Caenorhabditis species: Enhancing the Utility of C. elegans as a Model Organism. Natl Hum
689 Genome Res Inst White Pap. 2003 Oct 10;13.

690 38. Daugherty AC, Yeo RW, Buenrostro JD, Greenleaf WJ, Kundaje A, Brunet A. Chromatin
691 accessibility dynamics reveal novel functional enhancers in C. elegans. Genome Res. 2017
692 Dec;27(12):2096–107.

693 39. Jänes J, Dong Y, Schoof M, Serizay J, Appert A, Cerrato C, et al. Chromatin accessibility
694 dynamics across C. elegans development and ageing. eLife. 2018 Oct 26;7.

695 40. Murray JI, Boyle TJ, Preston E, Vafeados D, Mericle B, Weisdepp P, et al. Multidimensional
696 regulation of gene expression in the C. elegans embryo. Genome Res. 2012
697 Jul;22(7):1282–94.

698 41. Niu W, Lu ZJ, Zhong M, Sarov M, Murray JI, Brdlik CM, et al. Diverse transcription factor
699 binding features revealed by genome-wide ChIP-seq in C. elegans. Genome Res. 2011 Feb
700 1;21(2):245–54.

701 42. Araya CL, Kawli T, Kundaje A, Jiang L, Wu B, Vafeados D, et al. Regulatory analysis of the C.
702 elegans genome with spatiotemporal resolution. Nature. 2014 Aug 28;512(7515):400–5.

703 43. Slattery M, Riley T, Liu P, Abe N, Gomez-Alcala P, Dror I, et al. Cofactor binding evokes
704 latent differences in DNA binding specificity between Hox proteins. Cell. 2011 Dec
705 9;147(6):1270–82.

706 44. Abe N, Dror I, Yang L, Slattery M, Zhou T, Bussemaker HJ, et al. Deconvolving the
707 recognition of DNA shape from sequence. Cell. 2015 Apr 9;161(2):307–18.

708 45. Van Auken K, Weaver D, Robertson B, Sundaram M, Saldi T, Edgar L, et al. Roles of the
709 Homothorax/Meis/Prep homolog UNC-62 and the Exd/Pbx homologs CEH-20 and CEH-40
710 in C. elegans embryogenesis. Dev Camb Engl. 2002 Nov;129(22):5255–68.

711 46. Baugh LR, Wen JC, Hill AA, Slonim DK, Brown EL, Hunter CP. Synthetic lethal analysis of
712 Caenorhabditis elegans posterior embryonic patterning genes identifies conserved genetic
713 interactions. Genome Biol. 2005;6(5):R45.

714 47. Mace DL, Weisdepp P, Gevirtzman L, Boyle T, Waterston RH. A high-fidelity cell lineage
715 tracing method for obtaining systematic spatiotemporal gene expression patterns in
716 Caenorhabditis elegans. G3 Bethesda Md. 2013 May 20;3(5):851–63.

717 48. Narasimhan K, Lambert SA, Yang AWH, Riddell J, Mnaimneh S, Zheng H, et al. Mapping and
718 analysis of Caenorhabditis elegans transcription factor sequence specificities. eLife. 2015
719 Apr 23;4.

720 49. Tintori SC, Osborne Nishimura E, Golden P, Lieb JD, Goldstein B. A Transcriptional Lineage
721 of the Early C. elegans Embryo. Dev Cell. 2016 22;38(4):430–44.

722 50. Walton T, Preston E, Nair G, Zacharias AL, Raj A, Murray JI. The Bicoid class homeodomain
723 factors ceh-36/OTX and unc-30/PITX cooperate in C. elegans embryonic progenitor cells to
724 regulate robust development. PLoS Genet. 2015 Mar;11(3):e1005003.

725 51. Boeck ME, Boyle T, Bao Z, Murray J, Mericle B, Waterston R. Specific roles for the GATA
726 transcription factors end-1 and end-3 during C. elegans E-lineage development. Dev Biol.
727 2011 Oct 15;358(2):345–55.

728 52. Jin Y, Hoskins R, Horvitz HR. Control of type-D GABAergic neuron differentiation by C.
729 elegans UNC-30 homeodomain protein. Nature. 1994 Dec 22;372(6508):780–3.

730 53. Chang S, Johnston RJ, Hobert O. A transcriptional regulatory cascade that controls
731 left/right asymmetry in chemosensory neurons of C. elegans. Genes Dev. 2003 Sep
732 1;17(17):2123–37.

733 54. Lanjuin A, VanHoven MK, Bargmann CI, Thompson JK, Sengupta P. Otx/otd homeobox
734 genes specify distinct sensory neuron identities in C. elegans. Dev Cell. 2003 Oct;5(4):621–
735 33.

736 55. An JH, Vranas K, Lucke M, Inoue H, Hisamoto N, Matsumoto K, et al. Regulation of the
737 Caenorhabditis elegans oxidative stress defense protein SKN-1 by glycogen synthase
738 kinase-3. Proc Natl Acad Sci U S A. 2005 Nov 8;102(45):16275–80.

739 56. Bowerman B, Eaton BA, Priess JR. skn-1, a maternally expressed gene required to specify
740 the fate of ventral blastomeres in the early C. elegans embryo. Cell. 1992 Mar
741 20;68(6):1061–75.

742 57. Gilleard JS, McGhee JD. Activation of hypodermal differentiation in the Caenorhabditis
743 elegans embryo by GATA transcription factors ELT-1 and ELT-3. Mol Cell Biol. 2001
744 Apr;21(7):2533–44.

745 58. Ma X, Zhao Z, Xiao L, Xu W, Wang Y, Zhang Y, et al. Single-Cell Protein Atlas of
746 Transcription Factors Reveals the Combinatorial Code for Spatiotemporal Patterning the C.
747 elegans Embryo. bioRxiv. 2020 Jul 7;2020.06.30.178640.

748 59. Carroll SB. Evolution at two levels: on genes and form. PLoS Biol. 2005 Jul;3(7):e245.

749 60. Levine M. Transcriptional enhancers in animal development and evolution. Curr Biol CB.
750 2010 Sep 14;20(17):R754-763.

751 61. Cowing D, Kenyon C. Correct Hox gene expression established independently of position in
752 Caenorhabditis elegans. Nature. 1996 Jul 25;382(6589):353–6.

753 62. Dupuy D, Li Q-R, Deplancke B, Boxem M, Hao T, Lamesch P, et al. A First Version of the
754 Caenorhabditis elegans Promoterome. Genome Res. 2004 Oct 15;14(10b):2169–75.

755 63. Hunt-Newbury R, Viveiros R, Johnsen R, Mah A, Anastas D, Fang L, et al. High-throughput
756 in vivo analysis of gene expression in Caenorhabditis elegans. PLoS Biol. 2007
757 Sep;5(9):e237.

758 64. Reece-Hoyes JS, Shingles J, Dupuy D, Grove CA, Walhout AJM, Vidal M, et al. Insight into
759 transcription factor gene duplication from Caenorhabditis elegans Promoterome-driven
760 expression patterns. BMC Genomics. 2007 Jan 23;8:27.

761 65. Charest J, Daniele T, Wang J, Bykov A, Mandlbauer A, Asparuhova M, et al. Combinatorial
762 Action of Temporally Segregated Transcription Factors. Dev Cell. 2020 Nov 23;55(4):483-
763 499.e7.

764 66. Hong J-W, Hendrix DA, Levine MS. Shadow enhancers as a source of evolutionary novelty.
765 Science. 2008 Sep 5;321(5894):1314.

766 67. Frankel N, Davis GK, Vargas D, Wang S, Payre F, Stern DL. Phenotypic robustness conferred
767 by apparently redundant transcriptional enhancers. Nature. 2010 Jul 22;466(7305):490–3.

768 68. Perry MW, Boettiger AN, Bothma JP, Levine M. Shadow enhancers foster robustness of
769 Drosophila gastrulation. Curr Biol CB. 2010 Sep 14;20(17):1562–7.

770 69. Maduro MF. Gut development in C. elegans. Semin Cell Dev Biol. 2017 Jun;66:3–11.

771 70. Sarov M, Murray JI, Schanze K, Pozniakovski A, Niu W, Angermann K, et al. A genome-scale
772 resource for in vivo tag-based protein function exploration in C. elegans. Cell. 2012 Aug
773 17;150(4):855–66.

774 71. Green JL, Inoue T, Sternberg PW. Opposing Wnt pathways orient cell polarity during
775 organogenesis. Cell. 2008 Aug 22;134(4):646–56.

776 72. Fire A, Harrison SW, Dixon D. A modular set of lacZ fusion vectors for studying gene
777 expression in Caenorhabditis elegans. Gene. 1990 Sep 14;93(2):189–98.

778 73. Wei X, Potter CJ, Luo L, Shen K. Controlling gene expression with the Q repressible binary
779 expression system in Caenorhabditis elegans. Nat Methods. 2012 Mar 11;9(4):391–5.

780 74. Bao Z, Murray JI. Mounting Caenorhabditis elegans Embryos for Live Imaging of
781 Embryogenesis. Cold Spring Harb Protoc. 2011 Sep 1;2011(9):pdb.prot065599.

782 75. Boyle TJ, Bao Z, Murray JI, Araya CL, Waterston RH. AceTree: a tool for visual analysis of
783 Caenorhabditis elegans embryogenesis. BMC Bioinformatics. 2006 Jun 1;7:275.

784 76. Murray JI, Bao Z, Boyle TJ, Boeck ME, Mericle BL, Nicholas TJ, et al. Automated analysis of
785 embryonic gene expression with cellular resolution in C. elegans. Nat Methods. 2008
786 Jun;5(8):703–9.

787

788

789 ## Figure captions

790

791 **Figure 1: *ceh-13* and *nob-1/php-3* are expressed broadly in an overlapping pattern in the**
792 **early *C. elegans* embryo.** A) Time lapse images of transgenic *C. elegans* embryos carrying
793 two transgenes, a ubiquitous fluorescent histone to mark all nuclei (shown in green) and a
794 reporter of interest (shown in red), which can be a cis-regulatory element driving a fluorescent
795 histone (transcriptional) or a fluorescently tagged transcription factor protein (translational).
796 Image analysis software identifies nuclei, and quantifies reporter intensity within the nuclei,
797 which can be displayed as a lineage tree colored by expression as in (C). B) 3D projections of
798 nuclei expressing a CEH-13::GFP CRISPR reporter (red), NOB-1::GFP or PHP-3::GFP CRISPR
799 reporter (blue), with overlap shown in magenta, at 120 minutes (50 cell stage), 150 minutes
800 (100 cell stage), and 280 minutes (400 cell stage) post fertilization. NOB-1::GFP and PHP-
801 3::GFP CRISPR reporters were expressed in indistinguishable patterns (Supplemental Figure
802 1), but PHP-3::GFP was slightly brighter so is shown in the following panels. C) Lineage tree
803 though the 100-cell stage, showing early expression of CEH-13 and PHP-3 CRISPR reporters,
804 colored as in (B). D) Expressing lineages showing CEH-13 and/or PHP-3::GFP CRISPR
805 reporter expression to 350 minutes of development, colors as in (B). Note that CEH-13::GFP
806 precedes PHP-3::GFP and NOB-1::GFP in all lineages except ABp(l/r)papppp (asterisk -
807 expression is consistent in ABprpapppp and variable in ABplpapppp). (E-H) Quantitative detail
808 for highlighted lineages, showing nuclear fluorescence intensity of CEH-13::GFP (fosmid) and
809 NOB-1::GFP transgene reporters across developmental time for the cells leading to
810 ABp(l/r)appaaa (E), ABp(l/r)appppp (F), ABp(l/r)pppppppp (G), and Ep(l/r)p (H). For cell labels, x
811 = (l/r). Nuclear fluorescence intensity is in arbitrary units. Grey bars mark cell divisions.

812

813 **Figure 2: Regions upstream of *nob-1/php-3* can recapitulate its expression pattern.** A)
814 Genome browser view of the *nob-1*/*php-3* locus showing the genes (black), candidate
815 enhancers tested (brown), sequence conservation with other nematodes (grey), and NHR-2
816 ChIP-seq trace (dark blue) from modENCODE (42) and ATAC-seq traces (red:ABa lineage,
817 green: ABp lineage) from Charest et al, 2020 (65). B) Schematics of the *nob-1* reporter
818 constructs examined, shown in alignment with (A). Enhancers were primarily tested in an
819 orientation 5' to the *pes-10* minimal promoter, but a downstream orientation was also used for
820 the -4.3 kb enhancer. C) Lineage trees colored to show expression patterns for the various
821 reporters and tested enhancers with relevant reproducible activity, using a rainbow color scale
822 to increase visible dynamic range. Major expressing lineages are underlined: ABp(l/r)ap: pink,
823 ABp(l/r)ppp: cyan, Ep: black, Cpapp: orange, ectopic: purple. Note the changes in expression
824 driven by the -4.3 kb enhancer depending on its position relative to the *pes-10* minimal
825 promoter. D) Average nuclear fluorescence values for cells in the ABp(l/r)ap (pink) and
826 ABp(l/r)ppp (blue) lineages from at least four embryos, shown on a log scale. E) Ratio of
827 expression in average ABp(l/r)ap cell to the average ABp(l/r)ppp cell at the 350 cell stage for at
828 least 4 embryos. F) Lineage trees showing expression driven by the nob-1 -5.3 kb upstream
829 region reporter with the -3.4 and/or -4.3 enhancers are deleted. Lineages where expression is
830 lost are underlined with colors as in (C).
831
832 **Figure 3: Expression of cis-regulatory elements upstream of *nob-1* and *php-3* depends**
833 **on *ceh-13***. A) Fold change in expression level relative to mean wild-type control for *nob-1*
834 promoter and enhancers in *ceh-13* mutant and RNAi conditions. *P* values determined by
835 Wilcoxon Ranked Sum Test. B) Lineage view of wild-type *nob-1* -5.3kb upstream reporter
836 ("promoter") expression in specified lineages. C) -5.3kb *nob-1* promoter reporter expression in
837 *ceh-13(sw1)* null mutant.

838

839 **Figure 4: Hox co-factors precede *nob-1* and regulate its expression.** A) Trees of NOB-
840 1::GFP expressing lineages, ABp, E, and C, showing the expression of *ceh-13* (fosmid) and
841 *nob-1* (GFP transgene) reporters, and fosmid GFP transgene reporters for the Hox co-factors,
842 *ceh-20*, *ceh-40* and *unc-62*. Color thresholds were adjusted for each gene to show all
843 expressing cells. Highlighted branches are shown in graphs B, C and D. B-D) Average TF
844 reporter nuclear fluorescence intensity across embryos (n >= 2) and for left/right symmetric cells
845 across developmental time for the cells leading to B) ABp(l/r)apapa , C) ABp(l/r)pppaa and D)
846 Cpapp. Fluorescence intensity is in arbitrary units and grey bars mark cell divisions. E,F) Fold
847 change values for -5.3 kb *nob-1* promoter expression in untreated and *unc-62* RNAi treated (E)
848 or *ceh-40(gk159)* mutant embryos treated with *ges-1* (control) or *ceh-20* RNAi (F) in specified
849 lineages. Significant changes marked by asterisk; *P* values determined by Wilcoxon Ranked
850 Sum Test.

851

852 **Figure 5: *elt-1* regulates *nob-1* expression in ABp(l/r)ap lineage.** A) Partial lineage trees
853 showing ELT-1::GFP (Green), NOB-1::GFP (Blue) or overlapping (Cyan) expression in the ABp
854 and C lineages. Arrowheads indicate branches shown in subsequent panels. B-D) Average
855 ELT-1::GFP and NOB-1::GFP nuclear fluorescence intensity (arbitrary units) in cells leading to
856 B) ABp(l/r)apppap (neural fate) C), ABp(l/r)appppa (hypodermal fate), and D) Cpappd
857 (hypodermal fate). Grey bars mark cell divisions. E) Fold change values for the *nob-1* promoter
858 and -3.4 kb and -4.3 kb wild-type or mutated enhancers in the ABp(l/r)ap lineage in the control
859 and *elt-1(ok1002)* mutant conditions. F-G) Fold-change of *nob-1* reporter intensity in *elt-*
860 *1(ok1002)* relative to mean wild-type control level in the E) ABp(l/r)pp, F) ABp(l/r)ppp, and G)
861 Cpap lineages. *P* values determined by Wilcoxon Ranked Sum Test.

862

863 **Figure 6: Cell defects are observed in the posterior of both *ceh-13* and *nob-1* mutant**
864 **embryos.** A) Lineage showing *ceh-13* expression with plots of frequency of cell cycle defects
865 and cell position defects for each cell plotted below. Cells expressing *ceh-13* during their
866 development are highlighted in pink (ABalap and ABalpp, which express very low levels of CEH-
867 13::GFP, are denoted with lighter shading). Cell cycle defects are defined as missed, ectopic or
868 significant change in division timing of at least 5 minutes and cell position defects are defined as
869 significant deviation of at least 5 μm from the positions expected from wild type (see methods).
870 Defects are listed cumulatively for terminal cells, so defects in both a parent and daughter cell
871 would be scored as two defects. B) Lineage showing *nob-1* and *php-3* expression overlap with
872 plots of frequency of cell cycle defects and cell position defects for each cell plotted below. Cells
873 expressing both *nob-1* and *php-3* are highlighted in cyan on the plots. C, D) Plot of mean
874 deviation in microns vs. mean neighbor score for each cell in the embryo, colored by level of
875 NOB-1::GFP expression, for *nob-1(ct223)* mutant which disrupts both *nob-1* and *php-3* (C) and
876 wild-type (D) embryos. Neighbor score is a measure of whether a cell is close to its normal
877 neighbors; values above 0.8 indicate aberrant neighbor relationships. E, F) Plot of mean
878 deviation in microns vs. mean neighbor score for each cell in the embryo, colored by level of
879 CEH-13::GFP expression, for ceh-13(sw1) mutant (E) and wild-type (F) embryos. (G-I) Three-
880 dimensional plot of cell position deviations - arrows point from average wild-type location to
881 average mutant location for each cell, colors indicate the level of NOB-1::GFP (G) or CEH-
882 13::GFP(H-I) expression: G) *nob-1(ct223)* at 335 minutes of development. H) *ceh-13(sw1)* at
883 230 minutes of development) *ceh-13(sw1)* at 322 minutes of development. J) wild-type and *nob-*
884 *1(ct223)* mutant lineages for the ABp(l/r)ap and ABp(l/r)pp lineages, showing examples of cell
885 division defects. Green stars indicate the normal divisions of neuroblasts, orange Xs indicate the
886 failed divisions of these cells with the frequency observed noted below. Blue underline indicates
887 the expression of NOB-1::GFP. K) Wild-type and *ceh-13(sw1)* mutant lineages for the ABarp
888 lineage. Green stars indicate the normal development of ADEshL and H2L cells, orange Xs

889 indicate the ectopic division of these cells with the frequency observed noted below. Red
890 underline indicates the expression of CEH-13::GFP.
891
892 **Supplemental Figure 1: Hox gene are expressed in overlapping patterns.** A) Overlap in the
893 expression of NOB-1::GFP and PHP-3::GFP CRISPR knock-in alleles. Expression is nearly
894 identical except *php-3* is expressed more consistently in ABplpapppp. B, C) Early (B) and late
895 (C) overlap of a CEH-13::GFP fosmid translational reporter transgene with a -9kb NOB-1::GFP
896 rescuing translational reporter transgene. The expression patterns are nearly identical to the
897 CRISPR knock-in alleles except the 9kb NOB-1::GFP reporter has reduced expression in the C
898 lineage. D) Expression pattern of a CEH-13::GFP transgene that contains 8.2 kb of upstream
899 sequence plus the first intron. It lacks expression in the MS lineage compared to the other CEH-
900 13 reporters. E) Correlation between average CEH-13::GFP CRISPR and NOB-1::GFP CRISPR
901 reporters for each cell during embryonic development. F) Correlation between average CEH-
902 13::GFP CRISPR and NOB-1::GFP CRISPR reporters for each cell during embryonic
903 development. Note that no cells express high levels of both proteins. G) Correlation between
904 average CEH-13::GFP and PHP-3::GFP intensity levels for each cell at each (1.5 minute) time
905 point. Note that no cells express high levels of both proteins.
906
907 **Supplemental Figure 2: Some *nob-1* enhancer constructs drive variable ectopic**
908 **expression.** A) Representative examples showing the expression variability for each of the
909 enhancers tested. Colored lines indicate the lineages of interest. Some lineages with no
910 expression are shown as partial trees. B) Brightfield image of a hatched L1 larva carrying the
911 -4.3kb enhancer reporter and showing the “no backend” phenotype characteristic of *nob-1/php-*
912 *3* mutants. Nearby bead is 20μm in diameter.
913

914 **Supplemental Figure 3: *ceh-13* regulates enhancers of *nob-1*.** A) Graphs showing the effect
915 of *ceh-13* RNAi on NOB-1::GFP rescuing transgene as well as the control values for the *nob-1*
916 enhancer reporters (*sw1* mutant values same as reported in Fig. 3). Red * indicates p<0.05 in
917 Wilcoxon Ranked sum test. B) Lineage trees showing expression of the wild-type -3.4kb
918 enhancer and a version with mutated HOX sites.
919
920 **Supplemental Figure 4: Hox co-factors affect *nob-1* expression in specific lineages.** A)
921 Tree showing effects of *unc-62i* on *nob-1* promoter transcriptional reporter expression in the
922 ABpl lineage. Lineages with loss of expression are underlined. The ABp(l/r)apap lineage was
923 most affected in 13/14 lineages tested. B) Trees showing the effect of *unc-62i* on NOB-1::GFP
924 translational reporter expression, with two examples shown. Lineages affected are underlined.
925 C) Graphs for all embryos tested (eight) for the same lineages shown in (B). Red * indicates
926 p<0.05 in Wilcoxon Ranked sum test. D) Effect of *unc-62* RNAi on CEH-13::GFP fosmid
927 reporter in lineages where the two genes are both expressed. No significant changes were
928 detected.
929
930 **Supplemental Figure 5: Full Lineages for *nob-1* regulators.** Full lineages for CEH-20::GFP,
931 CEH-40::GFP, UNC-62::GFP, and ELT-1::GFP, all fosmid translational reporters. All lineages
932 are shown to at least the 350 cell stage - selected lineages are shown later to identify additional
933 expression or dynamics.
934
935 **Supplemental Figure 6: *nob-1* enhancer expression requires *elt-1*** A) Fold change values of
936 *nob-1* enhancers in control and *elt-1* mutant conditions in the ABp(l/r)ap and Cpap lineages (if
937 expressed in control). Mutant values are the same as reported in Fig. 5. Red * indicates p<0.05
938 in Wilcoxon Ranked sum test. B) Fold change values of *nob-1* enhancers in control and *elt-1*

939 mutant conditions in the ABp(l/r)ppp and Ep lineages (if expressed in control) where ELT-
940 1::GFP is not expressed. Red * indicates p<0.05 in Wilcoxon Ranked sum test. C) Expression of
941 the -3.4 kb enhancer and a version from which all GATA sites have been mutagenized in the
942 ABp, E and C lineages. Note: the mutagenesis also disrupted one *ceh-20/40* predicted site, two
943 *nob-1* predicted sites, and one *pop-1* predicted site, as these were fully overlapping with GATA
944 sites.
945
946 **Supplemental Figure 7: *ceh-36* and *unc-30* contribute to *nob-1* expression**. A) Wild-type
947 and *ceh-36(ok795);unc-30(ok613)* mutant embryos expressing the NOB-1::GFP reporter
948 transgene. Expression is shown in the ABp lineage at the ~200 cell stage. B) Boxplot showing
949 the ratio of expression in the ABp(l/r)ap lineage to the ABp(l/r)ppp lineage for wild-type and *ceh-*
950 *36(ok795);unc-30(ok613)* mutant at the 350 cell stage for at least 4 embryos. Red * indicates
951 p<0.05 in Wilcoxon Ranked sum test.
952
953 **Supplemental Figure 8: Defective positions of specific cells in *nob-1* mutants.** A) The
954 position of cells that normally express *nob-1* are highlighted in the context of the whole embryo
955 at ~320 minutes (~570 cells, early morphogenesis). As compared to the wild-type average (left),
956 the *nob-1(ct223)* mutant (right) cells are disorganized and displaced anteriorly, particularly
957 ABp(l/r)ppp and some ABp(l/r)app cells (ABp(l/r)appp). B) The positions of the SAB neuron and
958 neuroblasts (red) and DA motorneurons (blue) are shown relative to the intestine (green) in wild-
959 type (left) and *ceh-13(sw1)* mutant (right), showing the anterior displacement of these cells. C)
960 The positions of the neuroblasts that fail to divide the *nob-1(ct223)* mutant as compared to
961 control (left), showing that these are dramatically mispositioned.
962

963 **Supplemental Figure 9: Regulation of *nob-1/php-3* at the lineage and enhancer levels.** A)
964 Diagram summarizing the transcriptional regulation of *nob-1/php-3* expression in the specific
965 lineages noted. Asterisk indicates indirect regulation. Note: although *nob-1/php-3* are expressed
966 in other lineages in C, only Cpap was possible to analyze with the transgenic reporters
967 examined. Regulation by *pop-1/sys-1* from Zacharias et al., 2015 (Zacharias et al., 2015) B)
968 Diagram summarizing enhancer-level transcriptional regulation of *nob-1/php-3* by the indicated
969 factors. Specific enhancers regulated by *ceh-20/ceh-40*, *ceh-36/unc-30*, *pop-1/sys-1* and *unc-62*
970 were not defined, but their activity can be localized to the regions marked by brackets. Based on
971 our results, additional *cis*-regulatory elements likely exist within the blue, green and yellow
972 regions (yellow encompasses the rest of the genome).
973
974 **Supplemental Tables found in SupplementalTables1-10.xlsx**
975 Supplemental Table 1: Strain list
976 Supplemental Table 2: Tested enhancer sequences
977 Supplemental Tables 3-5: Motifs found in nob-1 enhancers -3.4kb, -4.3kb, -8.3kb
978 Supplemental Table 6: Cell averaged reporter values for all embryos analyzed
979 Supplemental Table 7: Number of embryos analyzed for each genotype/condition
980 Supplemental Tables 8-10: Cell division times for wild-type, *ceh-13(sw1),* and *nob-1(ct223)*
981 embryos
982
983 **Supplemental Tables 11-13**
984 Supplemental Table 11: Cell position values for control embryos
985 Supplemental Table 12: Cell position values for *ceh-13(sw1)* embryos
986 Supplemental Table 13: Cell position values for *nob-1(ct223)* embryos

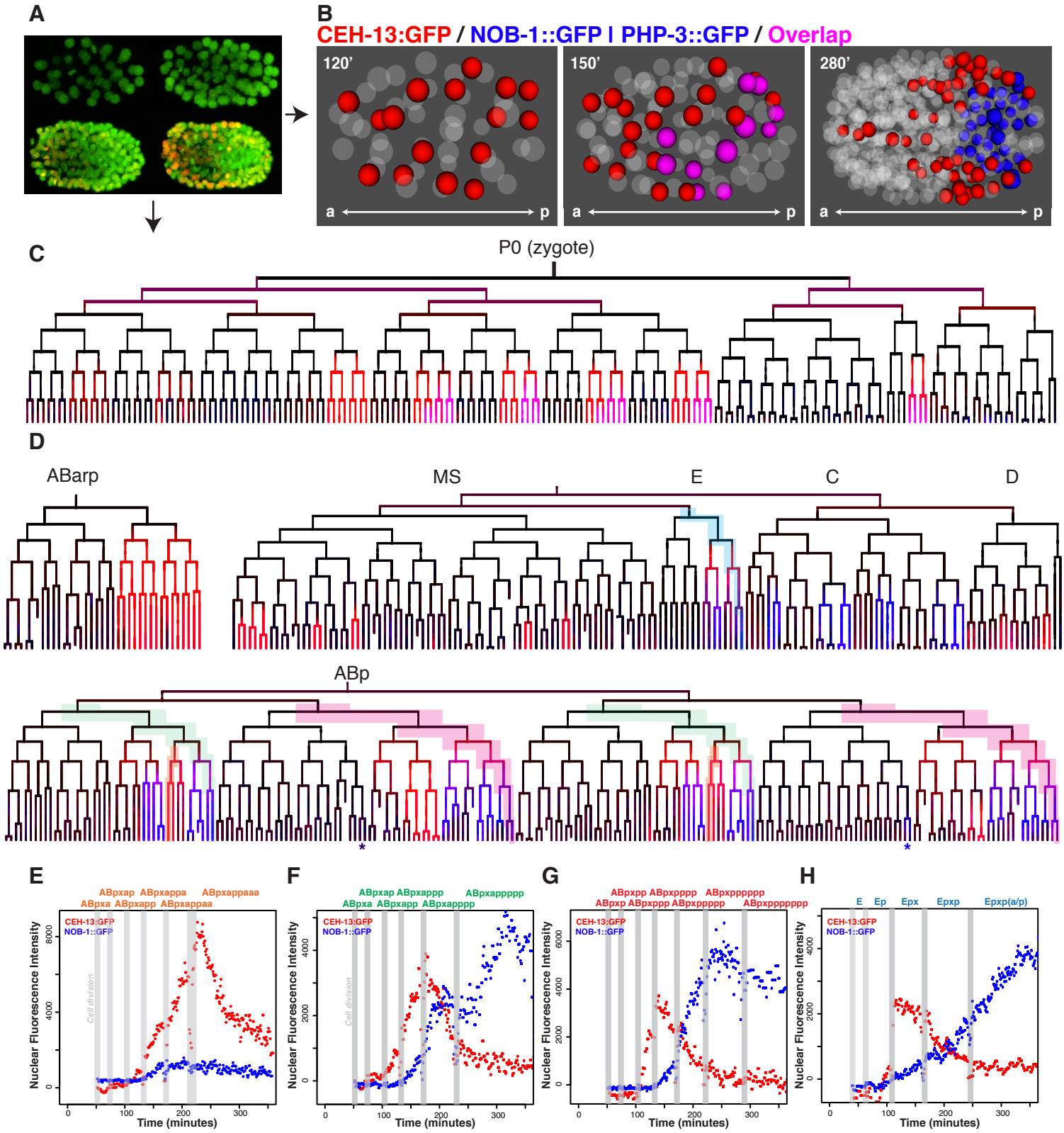
A
B
CEH-13:GFP / NOB-1::GFP I PHP-3::GFP / Overlap
120'
150'
280'
a
p
C
P0 (zygote)
D
ABarp
MS
E
C
D
ABp
E
ABpxap ABpxappa ABpxappaaa
ABpxa ABpxapp ABpxappaa
CEH-13:GFP
NOB-1::GFP
Cell division
Nuclear Fluorescence Intensity
Time (minutes)
F
ABpxap ABpxappp ABpxappppp
ABpxa ABpxapp ABpxappppp
G
ABpxpp ABpxpppp ABpxppppp
ABpxp ABpxppp ABpxpppp ABpxpppppp
H
E Ep Epx Epxp Epxp(a/p)

Figure 1

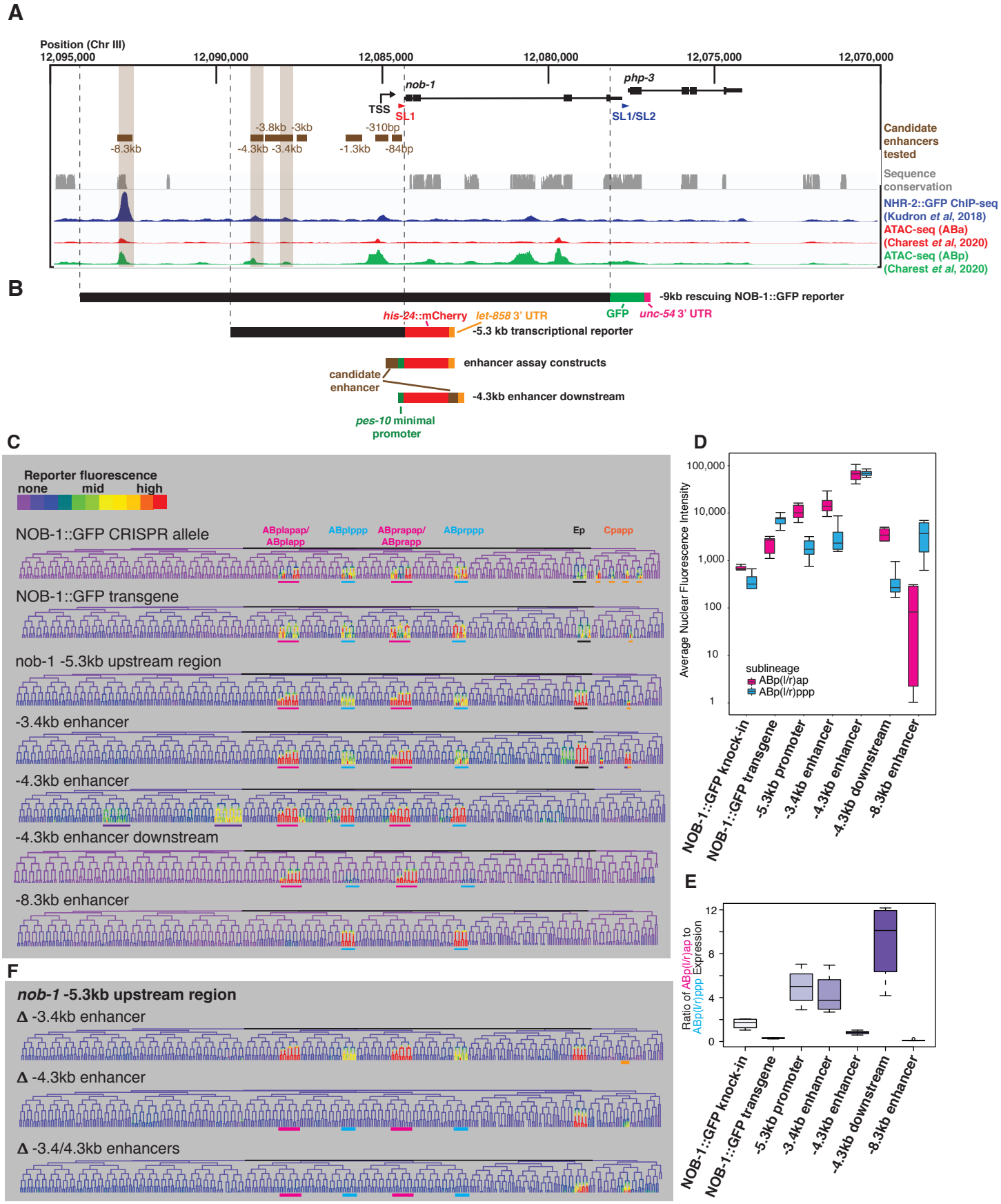
A
Position (Chr III)
12,095,000
12,090,000
12,085,000
12,080,000
12,075,000
12,070,000
nob-1
php-3
TSS
SL1
SL1/SL2
-8.3kb
-3.8kb
-3kb
-4.3kb
-3.4kb
-310bp
-1.3kb
-84bp
Candidate enhancers tested
Sequence conservation
NHR-2::GFP ChIP-seq (Kudron et al, 2018)
ATAC-seq (ABa) (Charest et al, 2020)
ATAC-seq (ABp) (Charest et al, 2020)
B
-9kb rescuing NOB-1::GFP reporter
his-24::mCherry
let-858 3' UTR
GFP
unc-54 3' UTR
-5.3 kb transcriptional reporter
enhancer assay constructs
candidate enhancer
-4.3kb enhancer downstream
pes-10 minimal promoter
C
Reporter fluorescence
none
mid
high
NOB-1::GFP CRISPR allele
ABplapap/ ABplapp
ABplppp
ABprapap/ ABprapp
ABprppp
Ep
Cpapp
NOB-1::GFP transgene
nob-1 -5.3kb upstream region
-3.4kb enhancer
-4.3kb enhancer
-4.3kb enhancer downstream
-8.3kb enhancer
D
Average Nuclear Fluorescence Intensity
100,000
10,000
1,000
100
10
1
sublineage
ABp(l/r)ap
ABp(l/r)ppp
NOB-1::GFP knock-in
NOB-1::GFP transgene
-5.3kb promoter
-3.4kb enhancer
-4.3kb enhancer
-4.3kb downstream
-8.3kb enhancer
E
Ratio of ABp(l/r)ap to ABp(l/r)ppp Expression
12
8
4
0
NOB-1::GFP knock-in
NOB-1::GFP transgene
-5.3kb promoter
-3.4kb enhancer
-4.3kb enhancer
-4.3kb downstream
-8.3kb enhancer
F
nob-1 -5.3kb upstream region
Δ -3.4kb enhancer
Δ -4.3kb enhancer
Δ -3.4/4.3kb enhancers

Figure 2

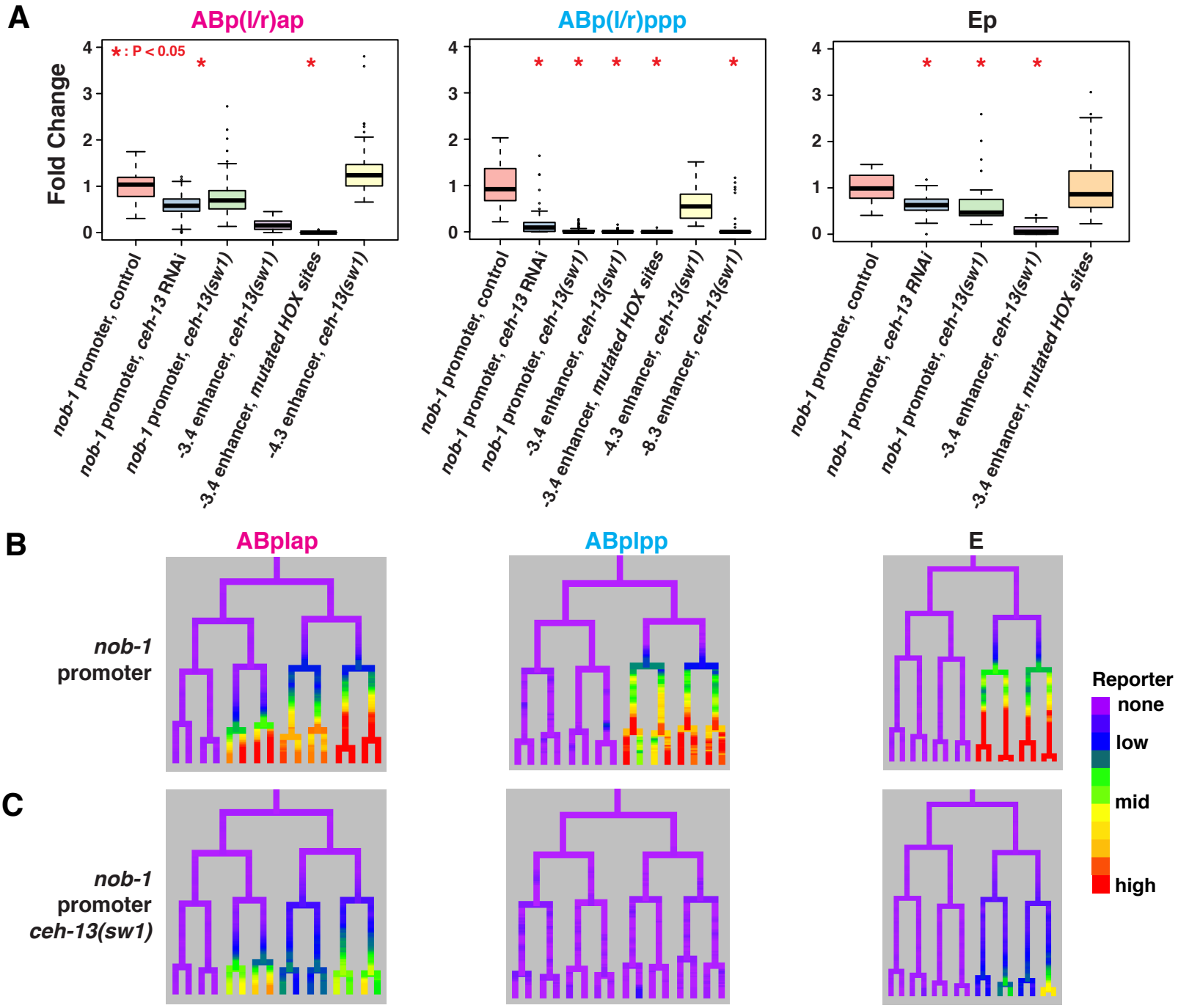
A
ABp(l/r)ap
ABp(l/r)ppp
Ep
Fold Change
* : P < 0.05
nob-1 promoter, control
nob-1 promoter, ceh-13 RNAi
nob-1 promoter, ceh-13(sw1)
-3.4 enhancer, ceh-13(sw1)
-3.4 enhancer, mutated HOX sites
-4.3 enhancer, ceh-13(sw1)
-8.3 enhancer, ceh-13(sw1)
B
ABplap
ABplpp
E
nob-1 promoter
C
nob-1 promoter ceh-13(sw1)
Reporter
none
low
mid
high

Figure 3

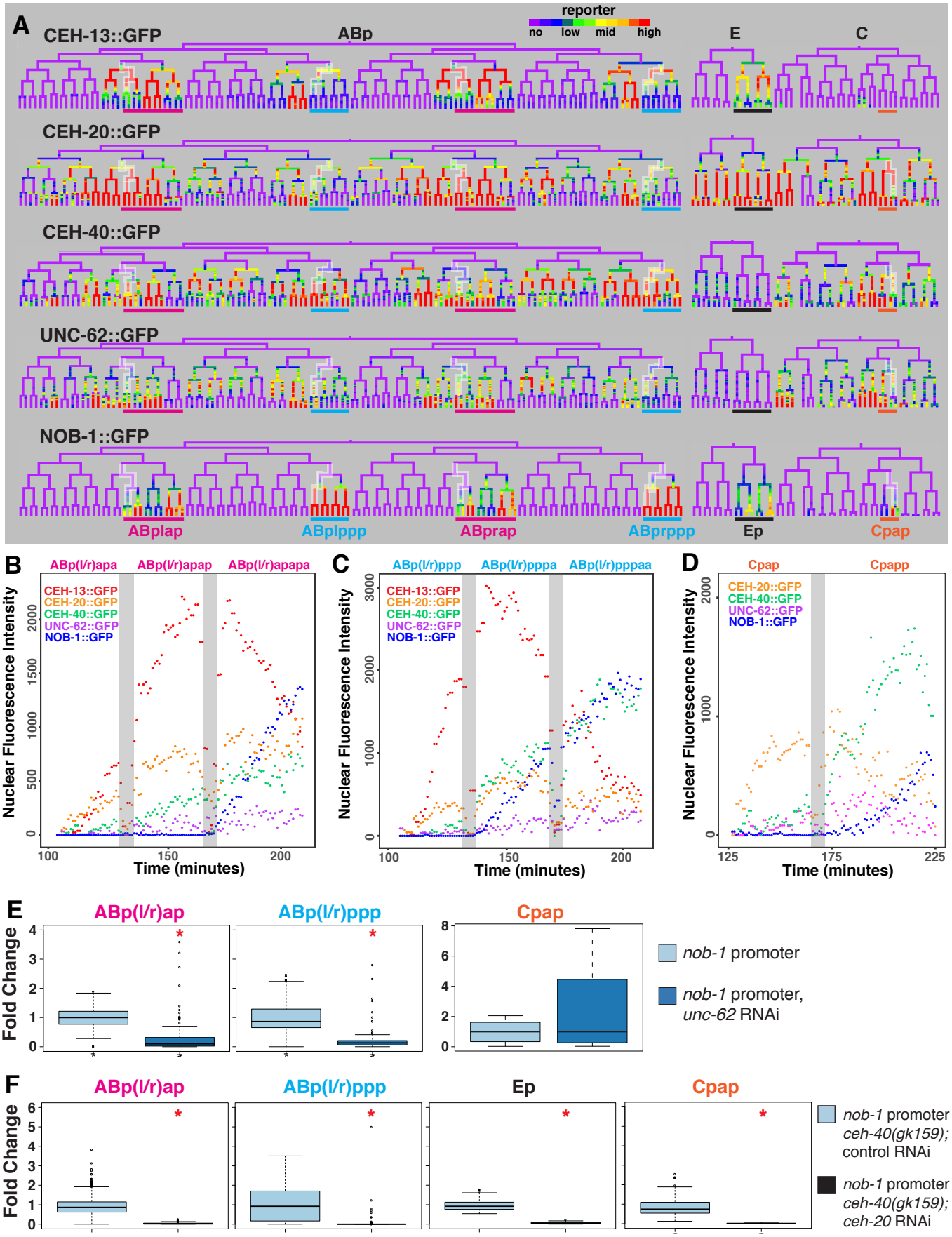
A
reporter
no
low
mid
high
CEH-13::GFP
ABp
E
C
CEH-20::GFP
CEH-40::GFP
UNC-62::GFP
NOB-1::GFP
ABplap
ABplppp
ABprap
ABprppp
Ep
Cpap
B
ABp(l/r)apa
ABp(l/r)apap
ABp(l/r)apapa
CEH-13::GFP
CEH-20::GFP
CEH-40::GFP
UNC-62::GFP
NOB-1::GFP
Nuclear Fluorescence Intensity
Time (minutes)
C
ABp(l/r)ppp
ABp(l/r)pppa
ABp(l/r)pppaa
D
Cpap
Cpapp
E
ABp(l/r)ap
ABp(l/r)ppp
Cpap
Fold Change
nob-1 promoter
nob-1 promoter, unc-62 RNAi
F
ABp(l/r)ap
ABp(l/r)ppp
Ep
Cpap
nob-1 promoter ceh-40(gk159); control RNAi
nob-1 promoter ceh-40(gk159); ceh-20 RNAi

Figure 4

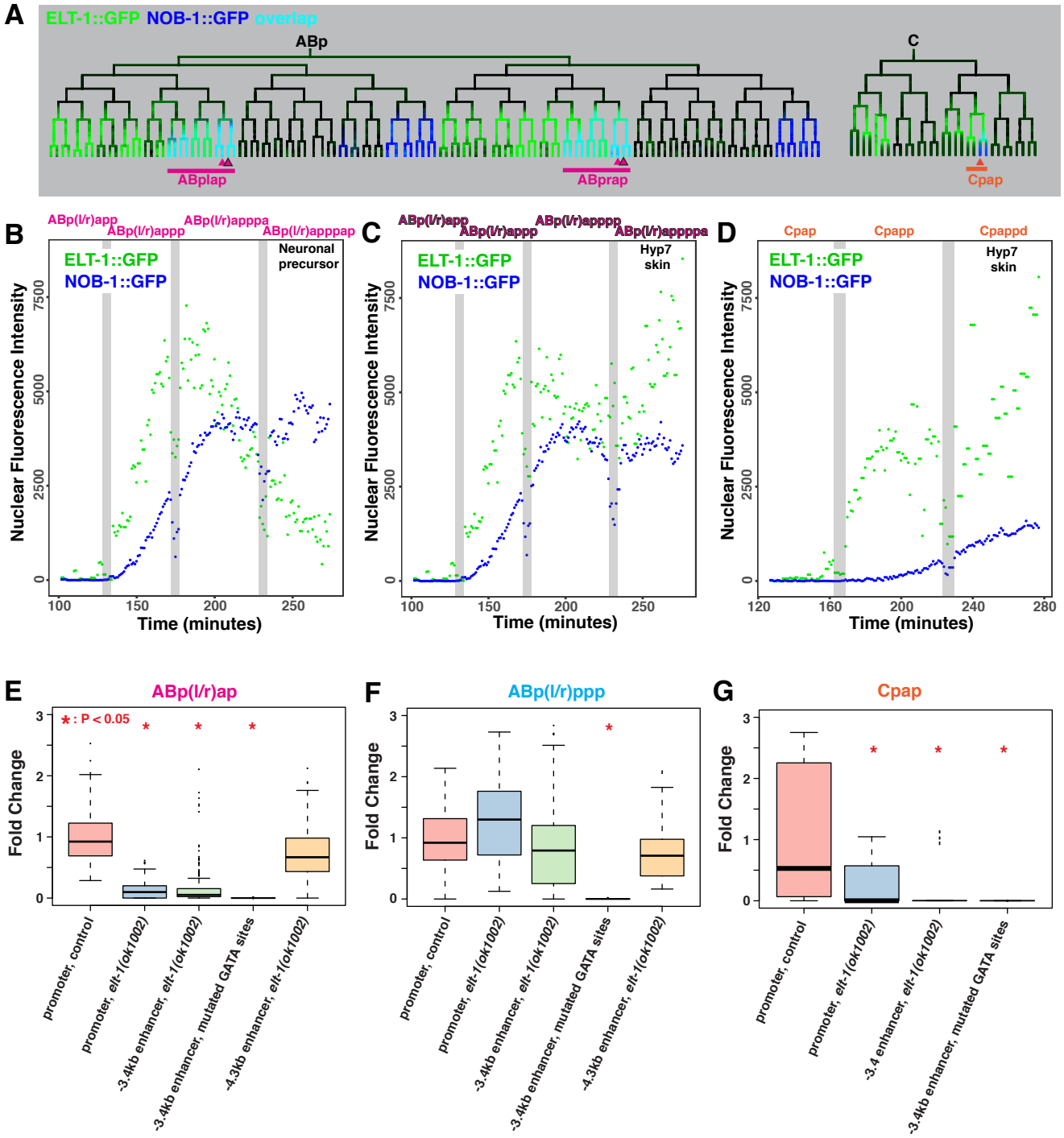
A
ELT-1::GFP NOB-1::GFP overlap
ABp
C
ABplap
ABprap
Cpap
B
ABp(l/r)app
ABp(l/r)appp
ABp(l/r)apppa
ABp(l/r)apppap
ELT-1::GFP
NOB-1::GFP
Neuronal precursor
Nuclear Fluorescence Intensity
Time (minutes)
C
ABp(l/r)app
ABp(l/r)appp
ABp(l/r)apppp
ABp(l/r)appppa
Hyp7 skin
D
Cpap
Cpapp
Cpappd
Hyp7 skin
E
ABp(l/r)ap
* : P < 0.05
Fold Change
promoter, control
promoter, elt-1(ok1002)
-3.4kb enhancer, elt-1(ok1002)
-3.4kb enhancer, mutated GATA sites
-4.3kb enhancer, elt-1(ok1002)
F
ABp(l/r)ppp
G
Cpap
-3.4 enhancer, elt-1(ok1002)

Figure 5

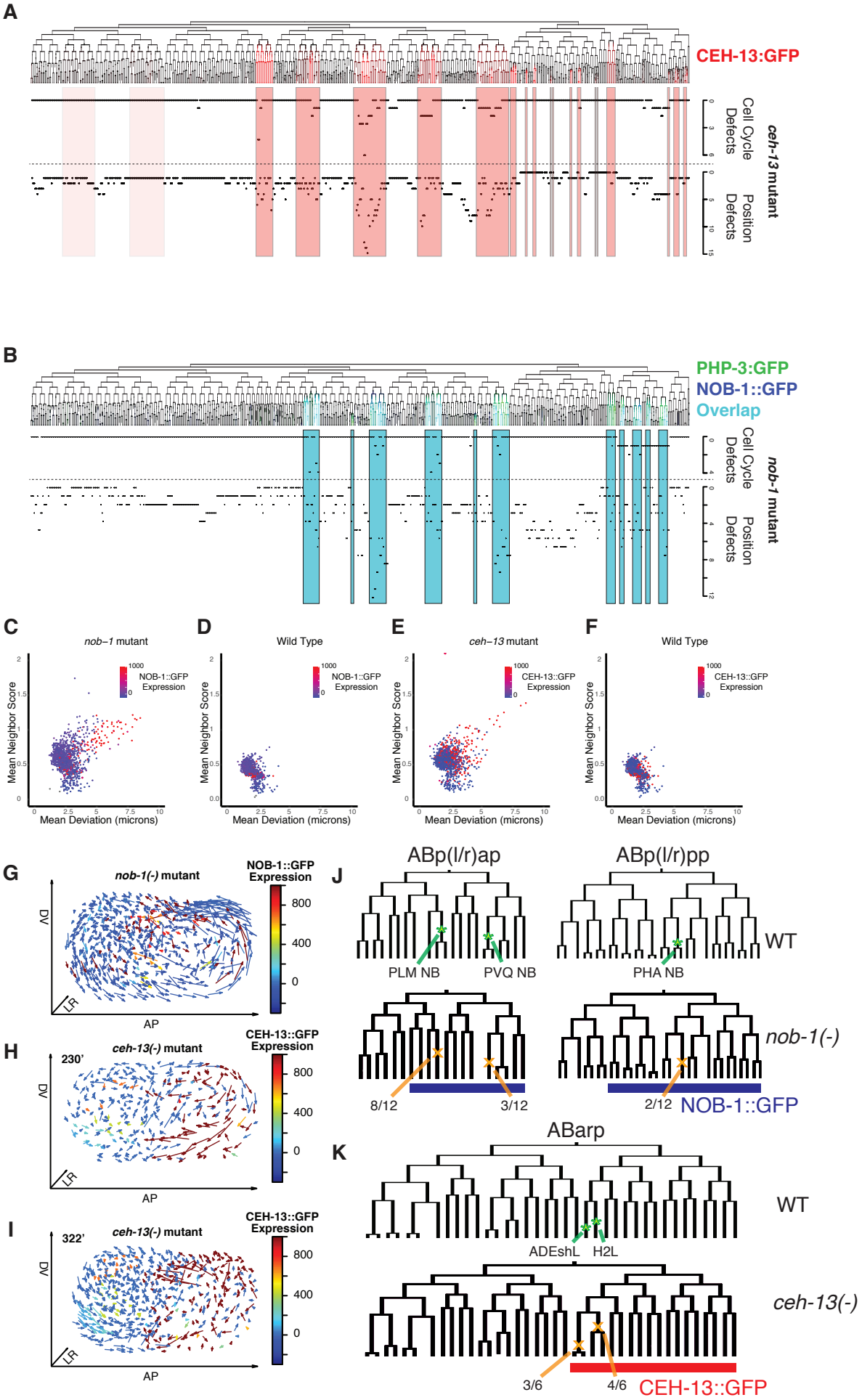
A
CEH-13:GFP
Cell Cycle Defects
Position Defects
ceh-13 mutant
B
PHP-3:GFP
NOB-1::GFP
Overlap
Cell Cycle Defects
Position Defects
nob-1 mutant
C
nob−1 mutant
NOB-1::GFP Expression
Mean Neighbor Score
Mean Deviation (microns)
D
Wild Type
NOB-1::GFP Expression
E
ceh−13 mutant
CEH-13::GFP Expression
F
Wild Type
CEH-13::GFP Expression
G
nob-1(-) mutant
NOB-1::GFP Expression
DV
LR
AP
H
ceh-13(-) mutant
230'
CEH-13::GFP Expression
I
ceh-13(-) mutant
322'
CEH-13::GFP Expression
J
ABp(l/r)ap
ABp(l/r)pp
PLM NB
PVQ NB
PHA NB
WT
nob-1(-)
8/12
3/12
2/12
NOB-1::GFP
K
ABarp
ADEshL
H2L
WT
ceh-13(-)
3/6
4/6
CEH-13::GFP

Figure 6

Figure S1

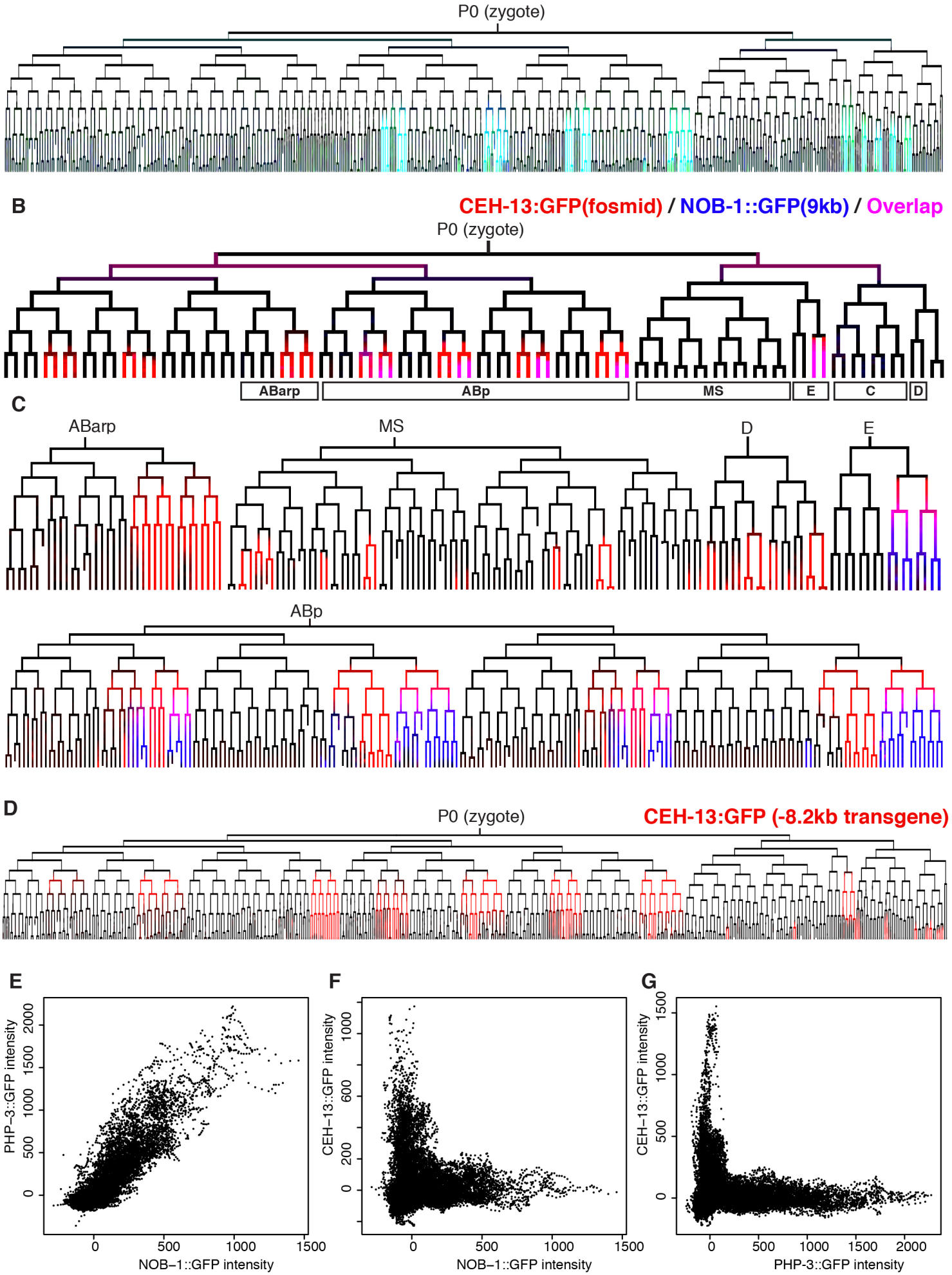
A
PHP-3:GFP / NOB-1::GFP / Overlap
P0 (zygote)
B
CEH-13:GFP(fosmid) / NOB-1::GFP(9kb) / Overlap
P0 (zygote)
ABarp
ABp
MS
E
C
D
C
ABarp
MS
D
E
ABp
D
P0 (zygote)
CEH-13:GFP (-8.2kb transgene)
E
PHP−3::GFP intensity
NOB−1::GFP intensity
F
CEH−13::GFP intensity
NOB−1::GFP intensity
G
CEH−13::GFP intensity
PHP-3::GFP intensity

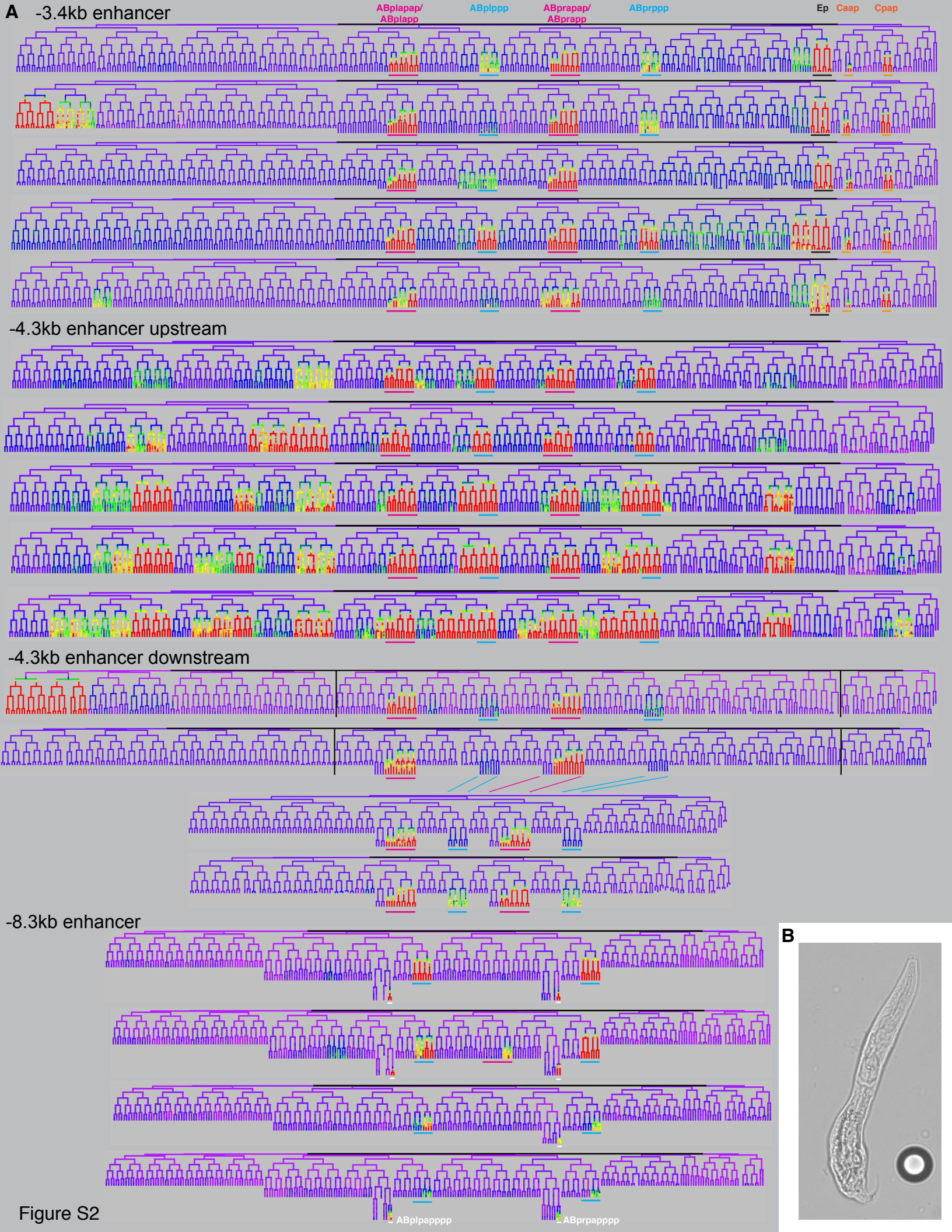
A
-3.4kb enhancer
ABplapap/
ABplapp
ABplppp
ABprapap/
ABprapp
ABprppp
Ep
Caap
Cpap
-4.3kb enhancer upstream
-4.3kb enhancer downstream
-8.3kb enhancer
ABplpapppp
ABprpapppp
B

Figure S2

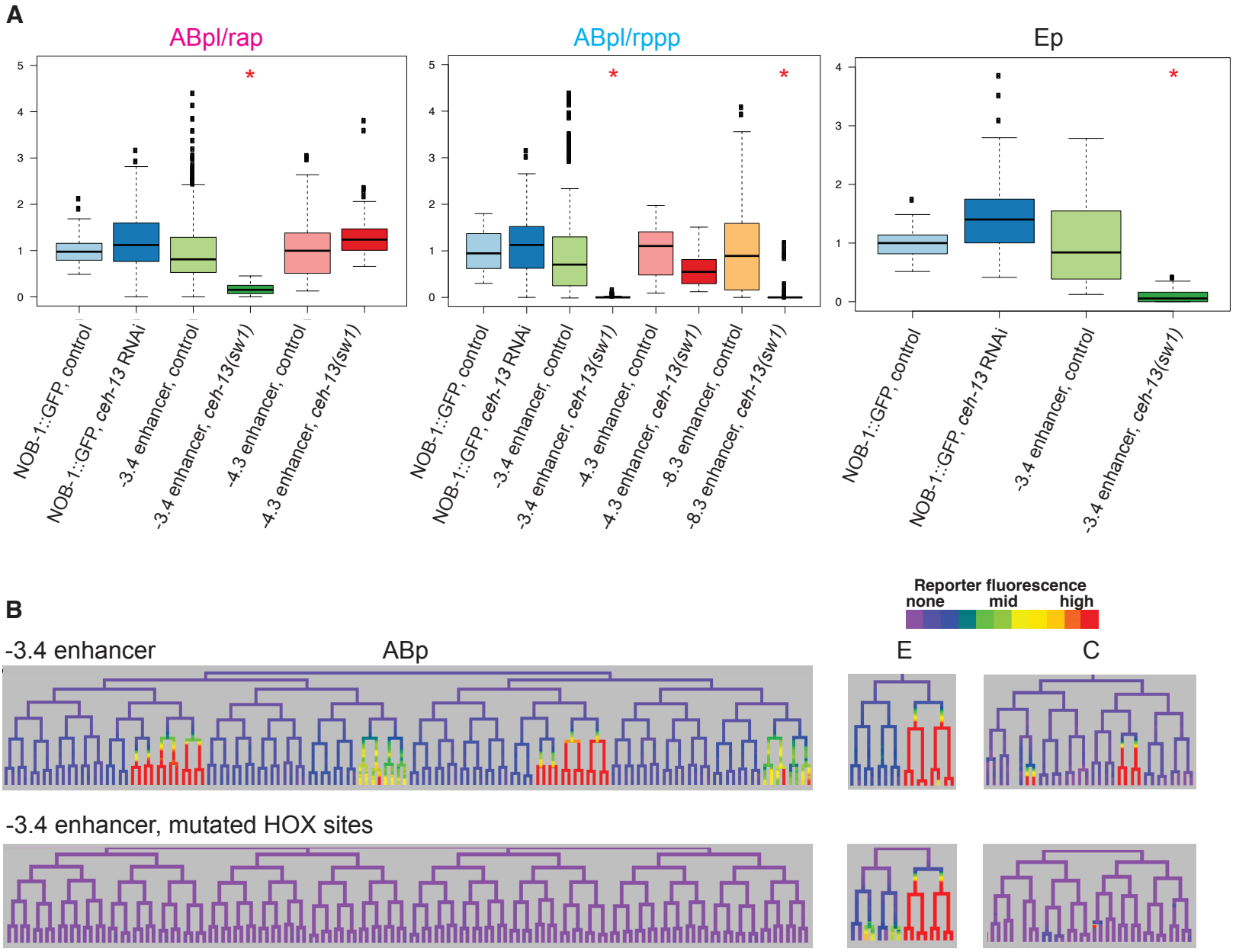
A
ABpl/rap
ABpl/rppp
Ep
NOB-1::GFP, control
NOB-1::GFP, ceh-13 RNAi
-3.4 enhancer, control
-3.4 enhancer, ceh-13(sw1)
-4.3 enhancer, control
-4.3 enhancer, ceh-13(sw1)
-8.3 enhancer, control
-8.3 enhancer, ceh-13(sw1)
B
Reporter fluorescence
none
mid
high
-3.4 enhancer
ABp
E
C
-3.4 enhancer, mutated HOX sites

Figure S3

Figure S4

A *nob-1* promoter, ABpl sublineage

control

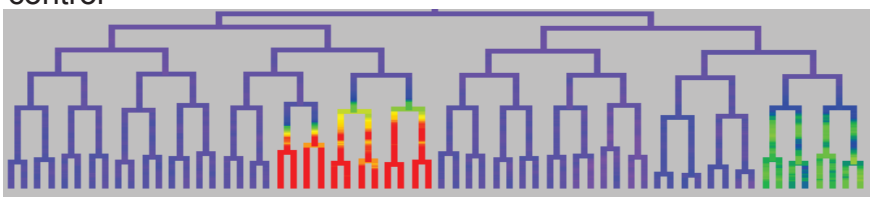

unc-62 RNAi

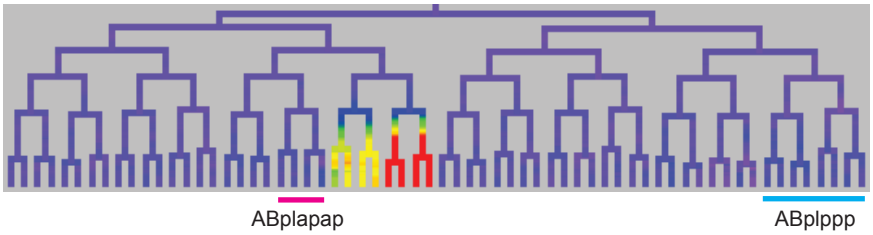

B NOB-1::GFP, ABpr sublineage

control

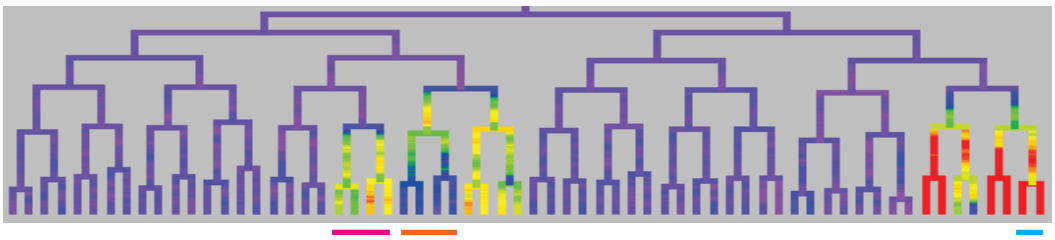

unc-62 RNAi

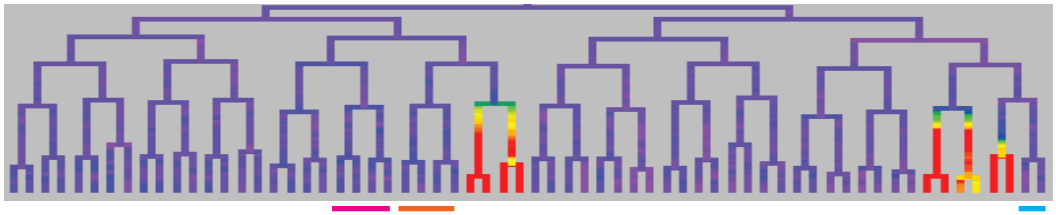

example #1

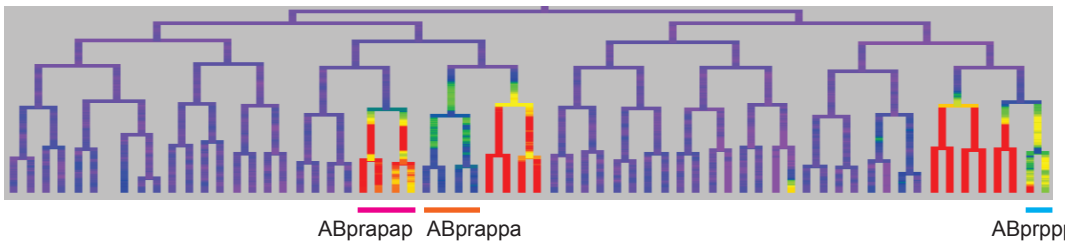

example #2

C

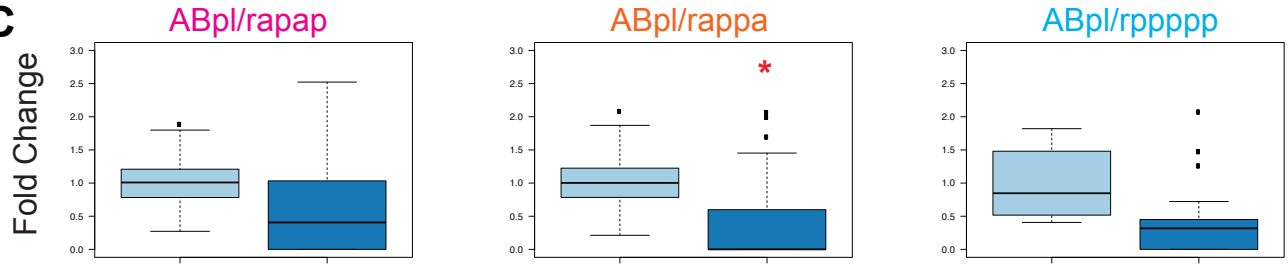

D

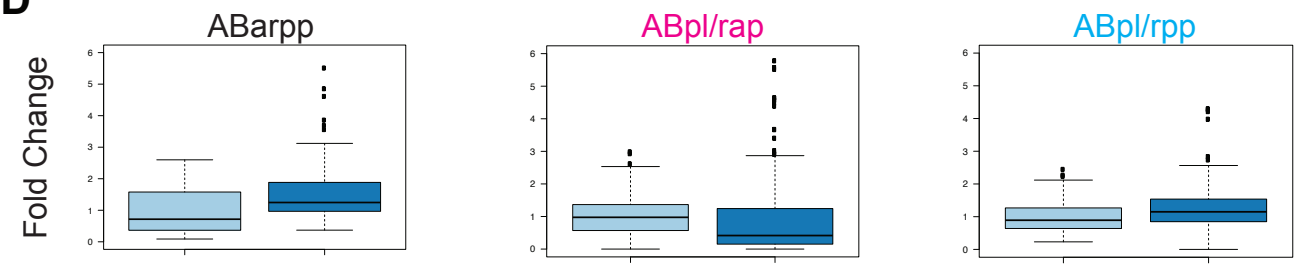

Figure S5

CEH-20::GFP

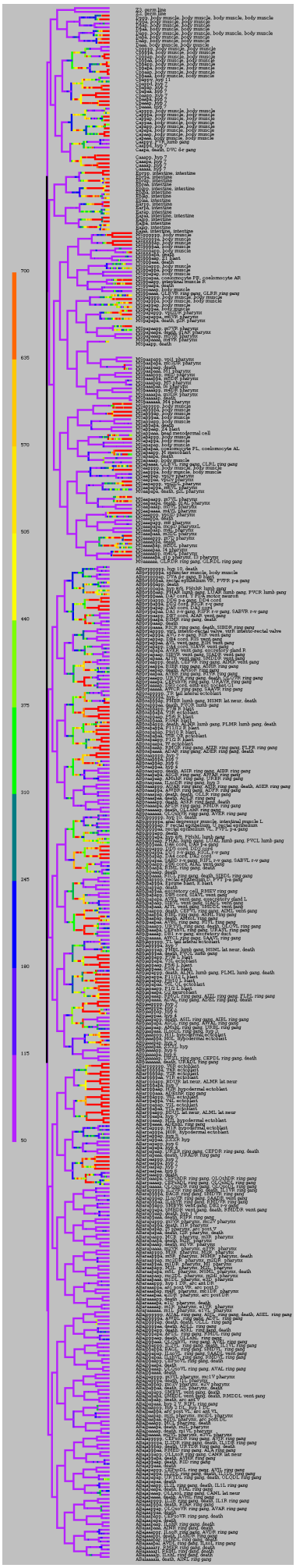

CEH-40::GFP

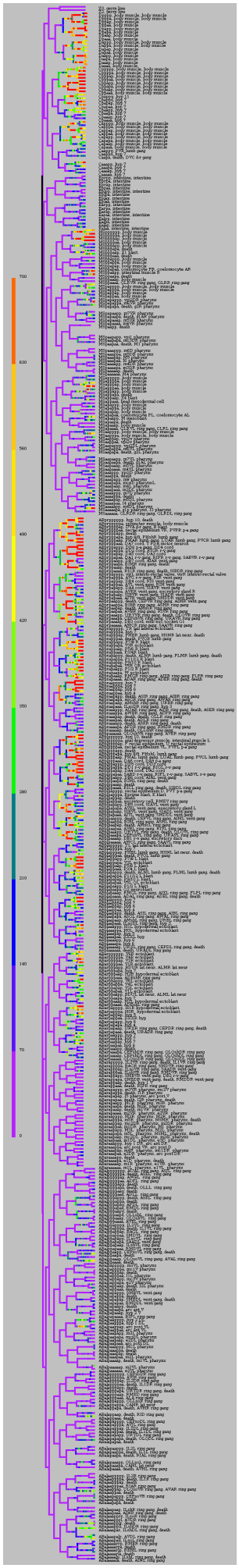

UNC-62::GFP

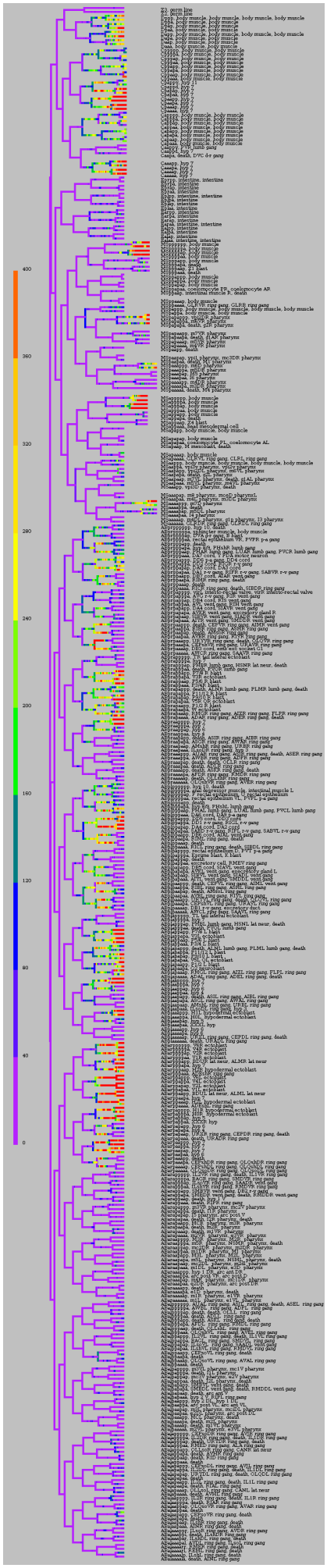

ELT-1::GFP

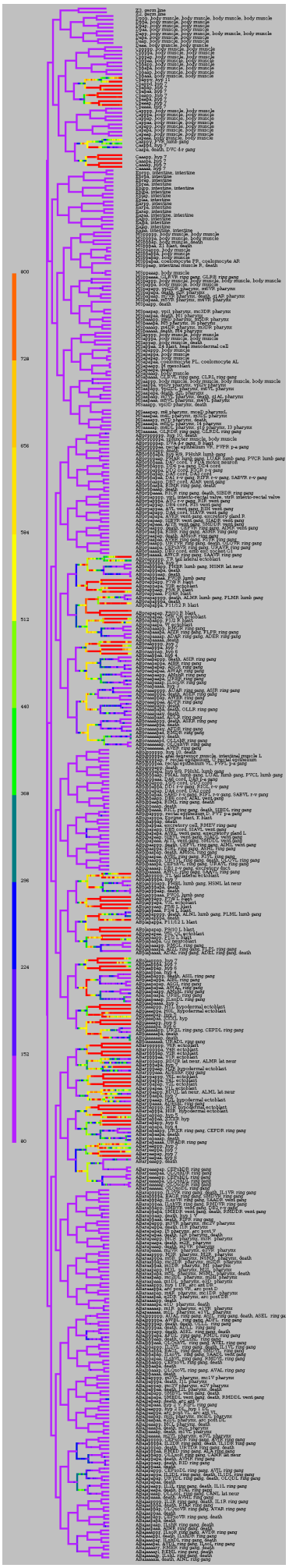

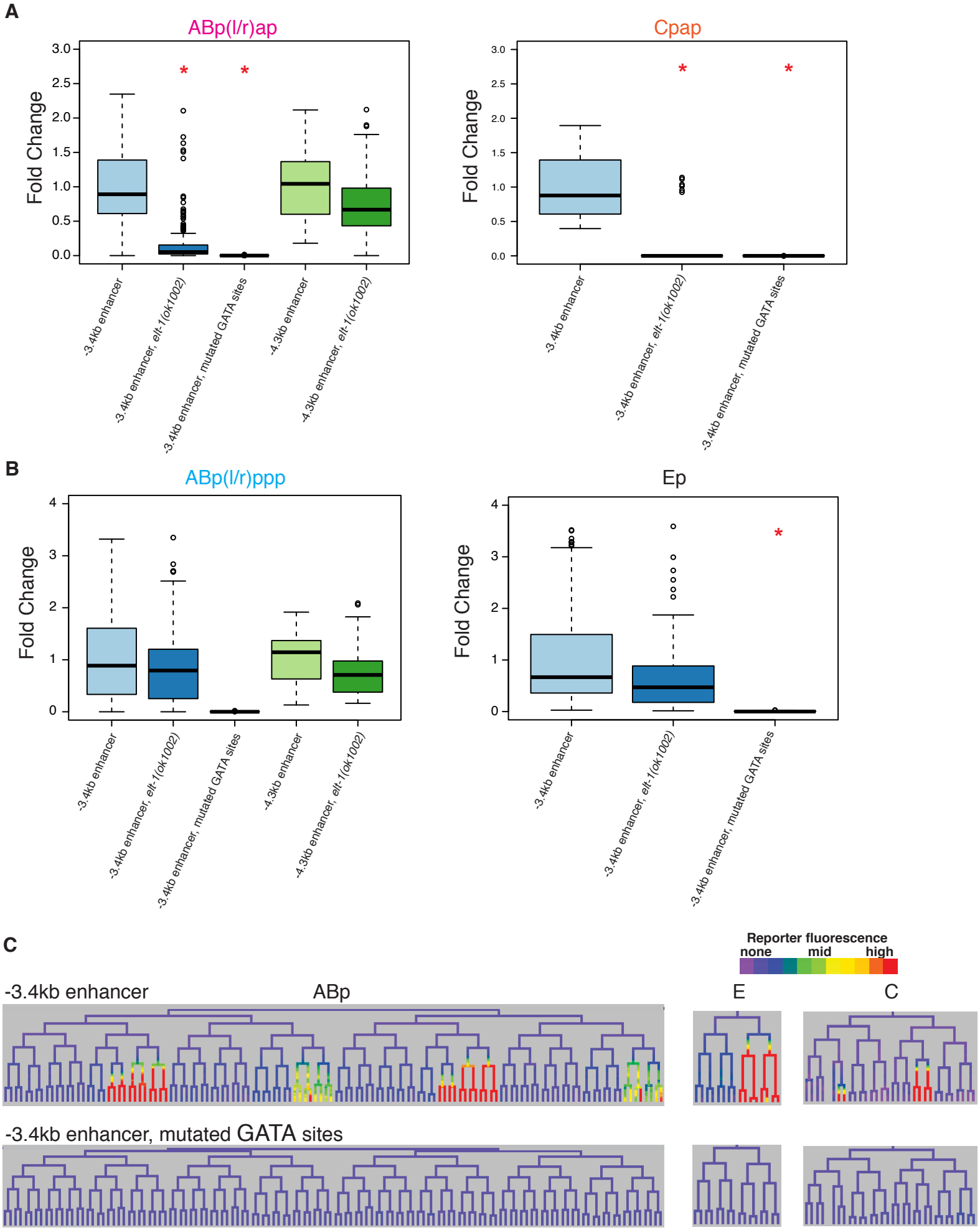
A
ABp(l/r)ap
Cpap
Fold Change
3.0
2.5
2.0
1.5
1.0
0.5
0.0
*
-3.4kb enhancer
-3.4kb enhancer, elt-1(ok1002)
-3.4kb enhancer, mutated GATA sites
-4.3kb enhancer
-4.3kb enhancer, elt-1(ok1002)
B
ABp(l/r)ppp
Ep
4
3
2
1
0
C
Reporter fluorescence
none
mid
high
-3.4kb enhancer
ABp
E
C
-3.4kb enhancer, mutated GATA sites

Figure S6

Figure S7

A

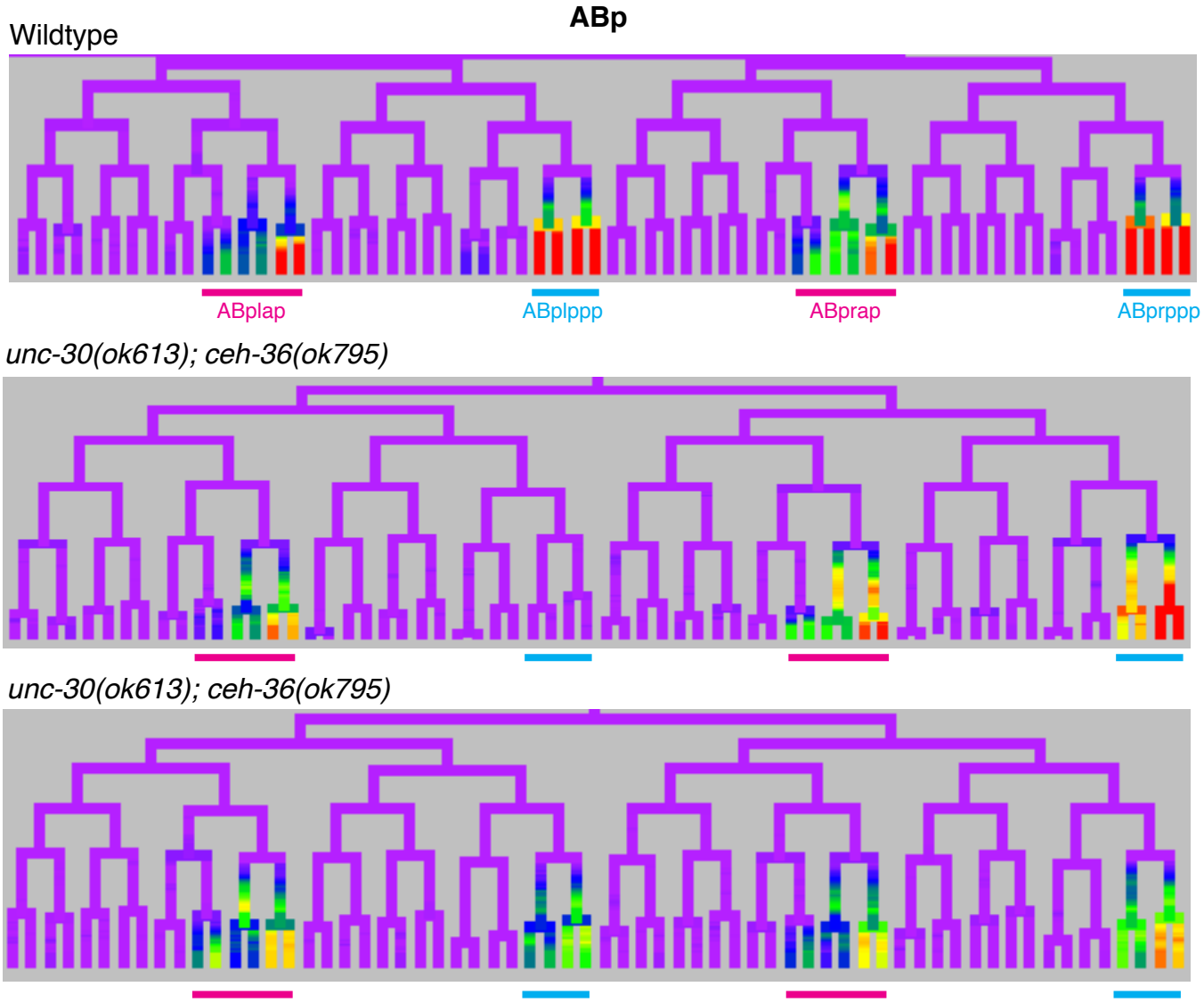
ABp
Wildtype
ABplap
ABplppp
ABprap
ABprppp
unc-30(ok613); ceh-36(ok795)
unc-30(ok613); ceh-36(ok795)

B

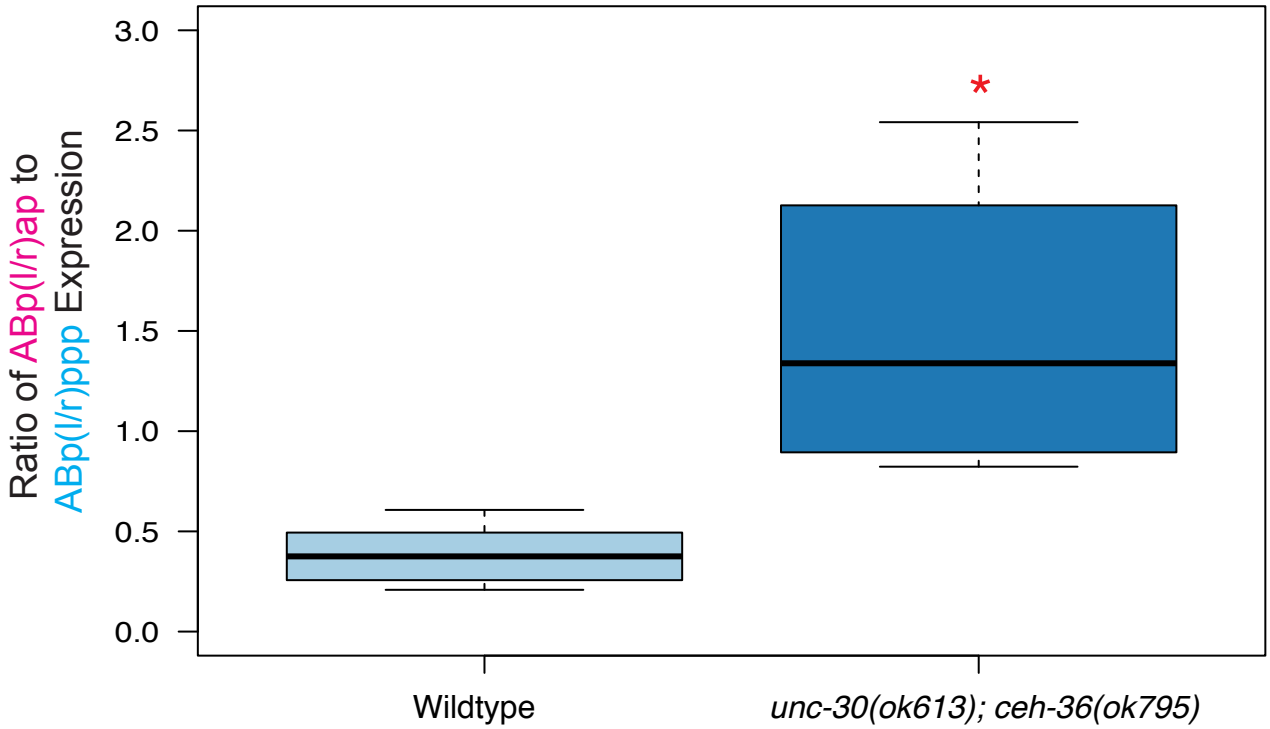
Ratio of ABp(l/r)ap to ABp(l/r)ppp Expression
3.0
2.5
2.0
1.5
1.0
0.5
0.0
*
Wildtype
unc-30(ok613); ceh-36(ok795)

A

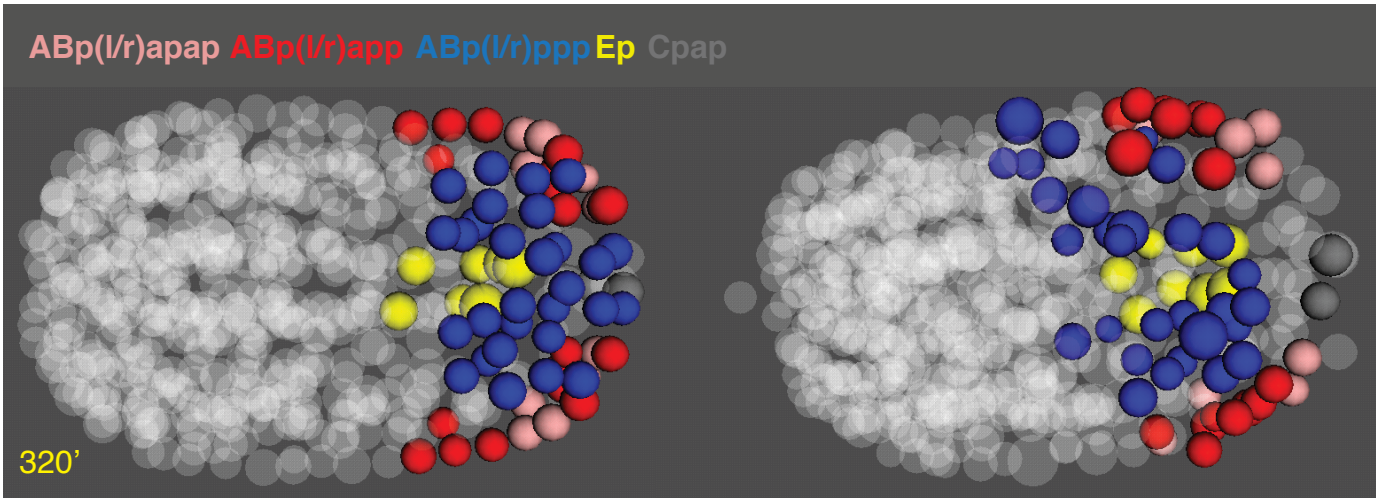

Wild Type ***nob-1(ct223)***

B

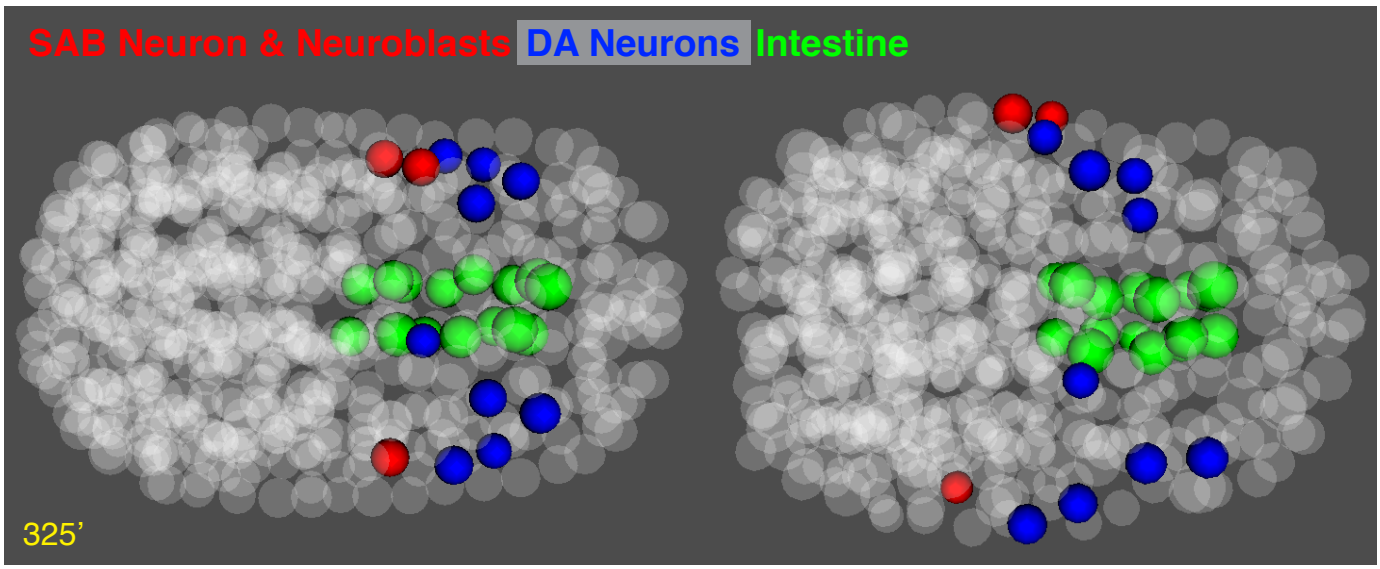

Wild Type ***ceh-13(sw1)***

C

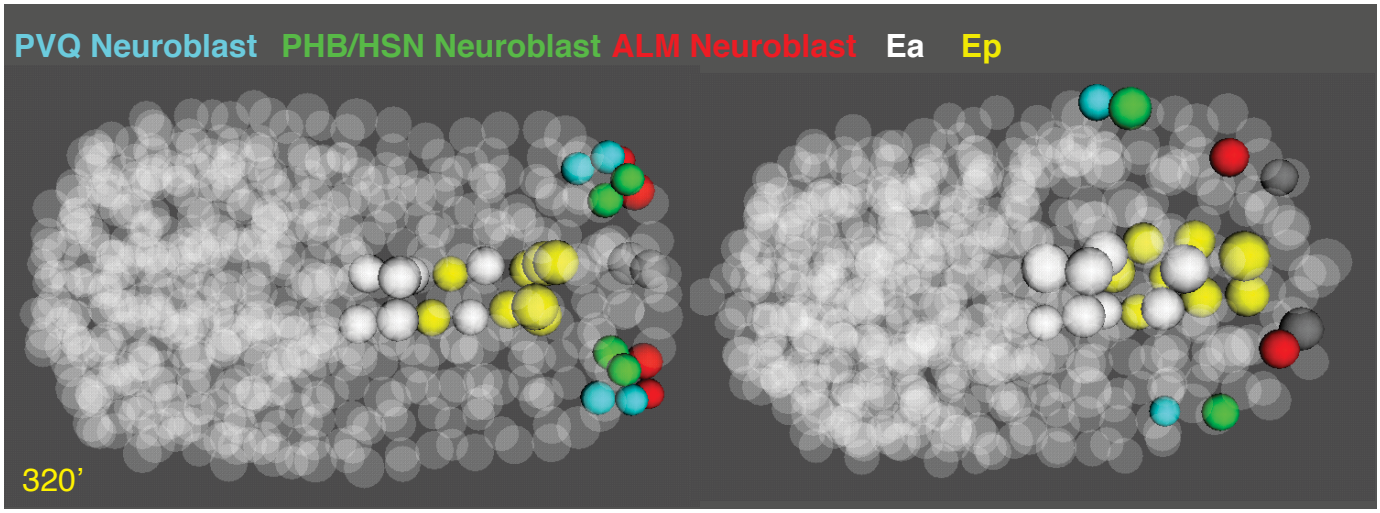

Wild Type ***nob-1(ct223)***

Figure S8

A Lineage level regulation

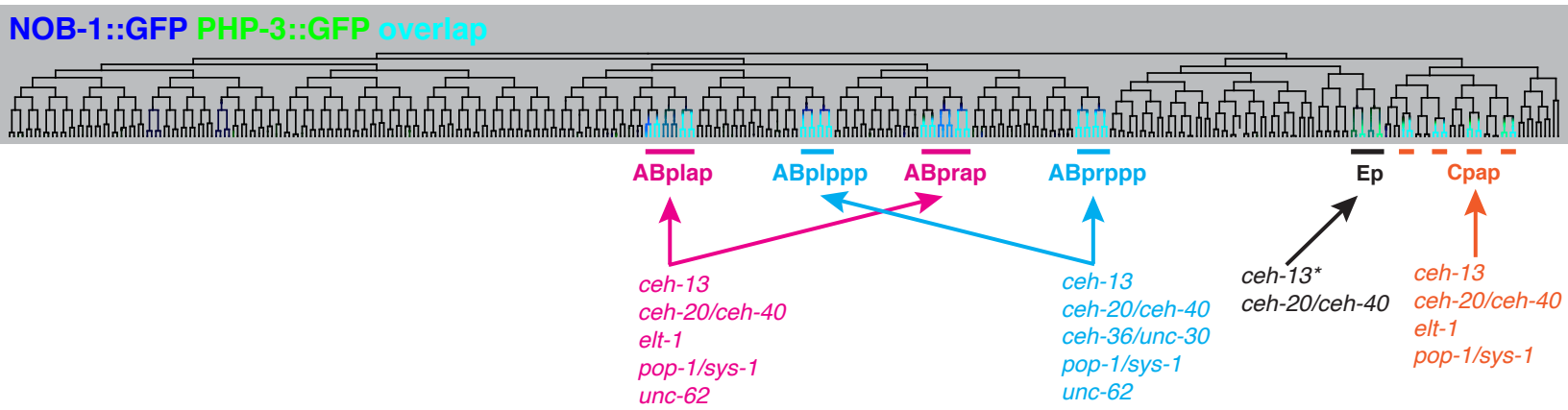

B Enhancer level regulation

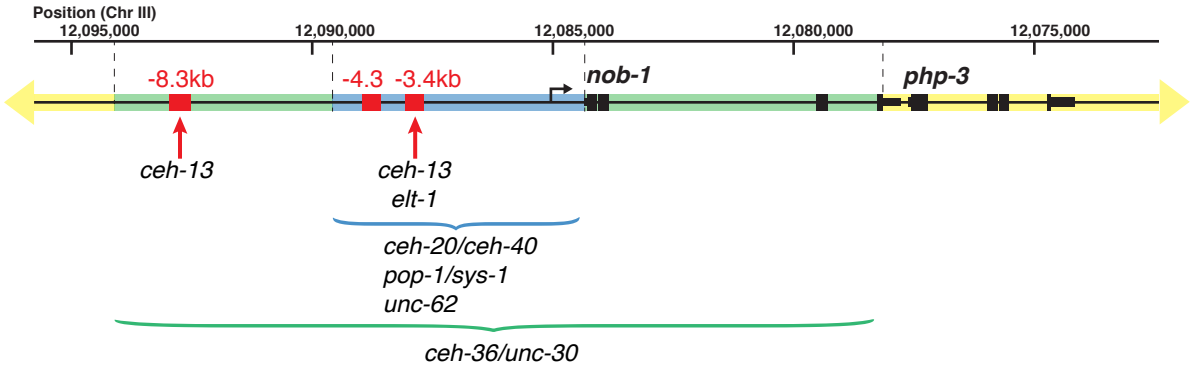

Figure S9